Swiss Permafrost Bulletin 2024

1 October 2023 to 30 September 2024
Annual report #6 on permafrost observations in the Swiss Alps
Swiss Permafrost Monitoring Network PERMOS
June 2025

Imprint

Publication of the Swiss Permafrost Monitoring Network (PERMOS).

Edited by

Jeannette Noetzli, PERMOS Office, WSL Institute for Snow and Avalanche Research SLF, Davos Dorf
Cécile Pellet, PERMOS Office, Department of Geosciences, University of Fribourg, Fribourg

Data collection

The seven PERMOS Partner Institutions are responsible for the maintenance of the field installations and data collection at the PERMOS sites: ETH Zurich (ETHZ), Universities of Fribourg (UniFR), Innsbruck (UIBK), Lausanne (UniL) and Zurich (UZH), University of Applied Sciences and Arts of Southern Switzerland (SUPSI), and WSL Institute for Snow and Avalanche Research SLF (WSL-SLF).

Author contributions

Jeannette Noetzli, WSL-SLF: Sections 1, 2, 3, 6, 7
Marcia Phillips, WSL-SLF: Section 6
Cécile Pellet, UniFR: Sections 1, 4, 5, 7

Reviewed by

Members of the PERMOS Scientific Committee: Chantal Del Siro, Reynald Delaloye, Isabelle Gärtner-Roer, Christian Hauck, Christin Hilbich, Christophe Lambiel, Coline Mollaret, Marcia Phillips, Samuel Weber.

Data availability

All PERMOS data are available online at https://www.permos.ch/data-portal and are subject to the PERMOS Data Policy (CC-BY 4.0). This report is based on the version 2025 of the PERMOS data set: https://doi.org/10.13093/permos-2025-01.

Citation

PERMOS 2025. Swiss Permafrost Bulletin 2024. Noetzli, J. and Pellet, C. (eds.). No. 6, 29 pp., doi.org/10.13093/permos-bull-2025.

Cover page

Rock glacier Muragl above Samedan in the Upper Engadine, GR. A replacement borehole was drilled in August 2024 to continue the long-term permafrost temperature measurements at the site. Photo: J. Noetzli.

List of abbreviations

ALT	Active Layer Thickness
ECV	Essential Climate Variable
ERT	Electrical Resistivity Tomography
ETHZ	ETH Zurich
FOEN	Federal Office for the Environment
GCOS	Global Climate Observing System
GCW	Global Cryosphere Watch
GFI	Ground Freezing Index
GNSS	Global Navigation Satellite System
GTI	Ground Thawing Index
GTN-P	Global Terrestrial Network for Permafrost
GST	Ground Surface Temperature
MAAT	Mean Annual Air Temperature
MAGST	Mean Annual Ground Surface Temperature
rMAGST	running Mean Annual Ground Surface Temperature
MeteoSwiss	Federal Office of Meteorology and Climatology MeteoSwiss
PERMOS	Swiss Permafrost Monitoring Network
RGV	Rock Glacier Velocity
RSF	Rock Slope Failure
SCNAT	Swiss Academy of Sciences
SLF	WSL Institute for Snow and Avalanche Research SLF
SUPSI	University of Applied Sciences and Arts of Southern Switzerland
TGS	Terrestrial Geodetic Survey
UIBK	University of Innsbruck
UniFR	University of Fribourg
UNIL	University of Lausanne
UZH	University of Zurich

Summary

The Swiss Permafrost Monitoring Network PERMOS has been documenting the state and changes of permafrost in the Swiss Alps for 25 years by field measurements of ground temperatures, electrical resistivities and rock glacier velocities. All observations show a consistent pattern of continued warming and permafrost degradation in the Swiss Alps since the start of PERMOS in 2000. The general trend is overlaid by inter-annual variations in response to annual meteorological conditions, particularly the timing and depth of the snow cover and air temperatures.

The hydrological year 2024 lasted from October 2023 to September 2024 and was the second warmest hydrological year in Switzerland above 1000 m asl. since the start of the measurements in 1864 with a mean annual air temperature 2.65 °C above the 1961–1990 average. The hydrological year 2024 was characterized by a very mild and snow-rich winter with early onset of the snow cover and above average snow heights in most regions, a cool and wet spring, and very warm atmospheric conditions in summer and autumn 2024.

As a result of the early snow cover and warm atmospheric conditions during autumn 2023 and winter 2024, the ground surface temperature remained at high levels. More than half of the sites reached new maximum values in 2024. The warm surface conditions resulted in record large active layer thicknesses, which were observed in all boreholes at the end of the thawing period. At a depth of 10 m temperature variations at the surface are measured with a delay of about half a year. Here, permafrost temperatures increased in 2024 compared to 2023 and reached new maximum values for most of the boreholes.

Measurements of permafrost electrical resistivity concur with the observed temperature increase. A considerable resistivity decrease was observed at the high-elevation bedrock site Stockhorn (–20% compared to 2023) and a smaller decrease at the talus slope Lapires (–7%) indicating an increase of the ratio between liquid water and ice content, which is considered a direct consequence of ground ice degradation. At Schilthorn, a resistivity increase was observed within the recently developed talik, pointing to a drying of the thaw layer at the site.

Rock glacier velocity in 2024 exhibited an increase at all surveyed sites compared to 2023 with an increase ranging from +5% at Gruben in the upper Valais to +77% at Hungerlitaelli in the same region. The average increase in the Swiss Alps was +39% compared to 2023. It can be attributed to the combined effect of warm conditions in the uppermost metres of the ground throughout the winter, which led to a smaller velocity decrease in winter compared to previous years, and high temperatures in summer.

The 2024 rockfall season began with a 5 Mio. m^3 rock slope failure at Piz Scerscen, which entrained large quantities of snow and ice and reached a runout length of over 5 km. After a quieter period, several events with volumes >100’000 m^3 were observed in the Alps in mid-August and autumn.

Overall, the permafrost observations during the hydrological year 2024 point to very warm and mostly record warm conditions in the Swiss Alps for all measured variables: ground surface temperatures, active layer thickness, permafrost temperature, permafrost resistivity and rock glacier velocity.

Zusammenfassung

Das Schweizer Permafrost-Beobachtungsnetz PERMOS dokumentiert seit 25 Jahren Zustand und Veränderungen des Permafrosts in den Schweizer Alpen anhand von Feldmessungen von Bodentemperaturen, elektrischem Widerstand und Blockgletscher-Geschwindigkeiten. Alle Beobachtungen zeigen ein konsistentes Bild anhaltende Erwärmung und Degradation des Permafrosts in den Schweizer Alpen seit dem Start von PERMOS im Jahr 2000. Der allgemeine Trend wird überlagert von inter-annuellen Variationen als Folge der jährlichen Witterungsbedingungen, insbesondere dem Zeitpunkt und der Mächtigkeit der Schneedecke und der Lufttemperaturen.

Das hydrologische Jahr 2024, das von Oktober 2023 bis September 2024 dauerte, war in der Schweiz oberhalb von 1000 m ü. M. das zweitwärmste hydrologische Jahr seit Beginn der Messungen im Jahr 1864 (das Kalenderjahr 2024 war das drittwärmste Jahr). Das Jahresmittel der Lufttemperatur lag 2.65 °C über dem 30-jährigen Mittel 1961–1990. Das hydrologische Jahr 2024 geprägt durch einen sehr milden und schneereichen Winter, einen kühlen und nassen Frühling und sehr warme atmosphärische Bedingungen im Sommer und Herbst 2024.

Infolge der frühen Schneedecke und der warmen atmosphärischen Bedingungen im Herbst 2023 und Winter 2024 blieb die Oberflächentemperatur am Boden auf hohem Niveau. Mehr als die Hälfte der Standorte erreichten im Jahr 2024 neue Höchstwerte. Die warmen Oberflächenbedingungen führten zu neuen Höchstwerten der Mächtigkeit der Auftauschicht, die am Ende der Tauperiode in allen Bohrlöchern beobachtet wurden. Temperaturschwankungen der Oberfläche werden in 10 m Tiefe einer Verzögerung von etwa einem halben Jahr gemessen. Hier stiegen die Permafrosttemperaturen im Jahr 2024 im Vergleich zu 2023 an und erreichten an den meisten Standorten neue Höchstwerte.

Die Messungen des elektrischen Widerstands im Permafrost stimmen mit dem beobachteten Temperaturanstieg überein. Ein grösserer Rückgang im Vergleich zum Vorjahr des spezifischen elektrischen Widerstands wurde am hochgelegenen Stockhorn (–20 % im Vergleich zu 2023) und ein kleinerer Rückgang in der Schutthalde Lapires (–7 %) beobachtet. Dies weist auf eine Zunahme des Verhältnisses zwischen Wasser- und Eisgehalt hinweist, was als direkte Folge des Rückgangs von Bodeneis interpretiert wird. Am Schilthorn wurde ein Anstieg des spezifischen Widerstands innerhalb des kürzlich entstandenen Taliks gemessen, was auf eine Abtrocknung des bereits aufgetauten Bodens an diesem Standort hinweist.

Die Geschwindigkeit der Blockgletscher nahm 2024 im Vergleich zu 2023 an allen vermessenen Standorten zu. Die Zunahme betrug zwischen +5% in Gruben im Oberwallis und +77% im Hungerlitaelli in derselben Region. Die durchschnittliche Zunahme in den Schweizer Alpen betrug +39% im Vergleich zu 2023. Sie wurde durch die warmen Bedingungen in den obersten Metern während des Winters 2024, welche die Geschwindigkeit im Winter weniger reduzierte als in den Vorjahren, und hohen Temperaturen im Sommer zurückgeführt werden.

Die Felssturzsaison 2024 begann mit dem 5 Mio. m³ grossen Felssturz am Piz Scerscen, der grosse Mengen an Schnee und Eis mitriss und eine Auslaufdistanz von über 5 km erreichte. Nach einer ruhigeren Periode wurden Mitte August und im Herbst mehrere Ereignisse mit >100'000 m3 in den Alpen beobachtet.

Insgesamt zeigen die Permafrostbeobachtungen im hydrologischen Jahr 2024 sehr warme Bedingungen in den Schweizer Alpen für alle Messgrössen und vielerorts neue Rekordwerte: Bodenoberflächentemperaturen, Mächtigkeit der Auftauschicht, Permafrosttemperatur, Permafrostwiderstand und Blockgletschergeschwindigkeit.

Résumé

Le réseau suisse d'observation du pergélisol PERMOS documente depuis 25 ans l'état et les changements du pergélisol dans les Alpes suisses à l'aide de mesures sur le terrain des températures du sol, de la résistivité électrique et de la vitesse des glaciers rocheux. Toutes les observations concordent et pointent vers un réchauffement et une dégradation générale du pergélisol depuis la création de PERMOS en 2000 même si d'importantes variations sont observées en réponse aux conditions météorologiques annuelles, et en particulier aux températures de l'air et conditions d'enneigement.

L'année hydrologique 2024, qui s'est étendue d'octobre 2023 à septembre 2024, a été la deuxième année hydrologique la plus chaude au-dessus de 1000 m d'altitude en Suisse depuis le début des mesures en 1864, avec une moyenne annuelle de la température de l'air supérieure de 2.65°C à la moyenne de 1961–1990. L'année hydrologique 2024 a été caractérisée par un hiver très doux et riche en neige, un printemps frais et humide, et des conditions atmosphériques très chaudes en été et en automne 2024. En raison de l'arrivée précoce de la neige et des conditions atmosphériques chaudes de l'automne 2023 et de l'hiver 2024, la température de la surface du sol est restée élevée. Plus de la moitié des sites ont atteint des nouvelles valeurs maximales en 2024. Ces conditions de surface très chaudes ont entraîné des épaisseurs record de la couche active, qui ont pu être observées dans tous les forages à la fin de la période de dégel. Au Schilthorn, le sol a dégelé jusqu'à environ 15 m de profondeur, ce qui a entraîné la création d'un talik au-dessus du pergélisol. À une profondeur de 10 m, les signaux de température de la surface sont mesurés avec un retard d'environ six mois. Ici, les températures du pergélisol ont augmenté en 2024 par rapport à 2023 et ont atteint de nouvelles valeurs maximales pour la plupart des forages.

Les mesures de la résistivité électrique du pergélisol concordent avec l'augmentation observée des températures du sol. Une diminution considérable de la résistivité a été observée sur le plateau rocheux de haute altitude de Stockhorn (–20% par rapport à 2023) et une diminution plus faible sur l'éboulis de Lapires (–7%). Cela indique une augmentation du rapport entre la teneur en eau liquide et en glace, considérée comme une conséquence directe de la fonte de la glace du pergélisol. Au Schilthorn, une augmentation de la résistivité a été observée dans le talik récemment formé, indiquant un assèchement de la partie dégelée du sol sur ce site.

La vitesse des glaciers rocheux a augmenté sur tous les sites étudiés par rapport à 2023, avec des valeurs allant de +5% à Gruben dans le Haut-Valais à +77% à Hungerlitaelli dans la même région. L'augmentation moyenne dans les Alpes suisses était de +39% par rapport à 2023. Elle peut être attribuée à l'effet combiné des conditions chaude du sol tout au long de l'hiver, ce qui a conduit à une diminution hivernale moins prononcée par rapport aux années précédentes et à des températures élevées en été.

Au niveau des instabilités de versant, la saison 2024 a commencé par un éboulement de 5 millions de mètres cubes au Piz Scerscen, entraînant de grandes quantités de neige et de glace, avec une sortie de plus de 5 km. Après une période plus calme, les chutes de pierres ont repris à la mi-août et à l'automne avec plusieurs événements plus importants (>100'000 m3) dans les Alpes.

Dans l'ensemble, les observations au cours de l'année hydrologique 2024 indiquent des conditions de pergélisol très chaudes, voire records, dans les Alpes suisses pour toutes les variables mesurées: températures de surface du sol, épaisseur de la couche active, température du pergélisol, résistivité électrique du pergélisol et vitesse des glaciers rocheux.

Contents

1 Introduction

The Swiss Permafrost Monitoring Network (PERMOS, www.permos.ch) has been documenting the state and evolution of permafrost in the Swiss Alps based on field measurements since 2000. Results have been compiled annually in the *Swiss Permafrost Bulletin* since 2019. Regular reporting on permafrost conditions is based on hydrological years because the snow cover has an important influence on the permafrost conditions. This bulletin documents the results of permafrost observations in the Swiss Alps during the hydrological year 2024, which runs from 1 October 2023 to 30 September 2024.

Permafrost is a key component of the mountain cryosphere and is defined as ground that remains at or below 0 °C for at least two consecutive years. In the Swiss Alps, it typically occurs at elevations above ca. 2200 m asl. and underlies 3–5% of the Swiss territory. Permafrost exists hidden in bedrock and rock debris slopes of the high mountain areas. It is sensitive to changing atmospheric conditions and is recognized by the Global Climate Observing System (GCOS) of the World Meteorological Organization (WMO) as an Essential Climate Variable (ECV). Three key indicator variables – so-called ECV quantities – were defined (WMO 2022, WMO 2024): permafrost temperature, active layer thickness and rock glacier velocity. Internationally, permafrost observations are coordinated in the framework of the Global Terrestrial Network for Permafrost (GTN-P) (Streletskiy et al. 2021).

The PERMOS monitoring strategy is based on field measurements of three primary variables, aligning with and complementing the quantities associated with the ECV permafrost:

1) **Ground temperature** near the surface and at depth,
2) **Permafrost electrical resistivity**, and
3) **Rock glacier velocity**.

Direct observation of permafrost is carried out by continuous ground temperature measurements at multiple depths in boreholes down to 100 metres depth. These point measurements are supplemented by spatially distributed temperature recordings at the ground surface. Changes in the ground ice and water content are observed at permanently installed profiles at borehole locations using geoelectrical methods. Rock glacier velocities are determined using terrestrial geodetic surveys and permanently installed GNSS devices. The active layer thickness (ALT) is derived from the ground temperature time series. It is defined as the deepest seasonal penetration of the 0 °C isotherm. In the framework of PERMOS also the following data and information are collected:

4) **Meteorological data** with automatic weather stations at selected borehoe sites, and
5) **Rock Slope Failure (RSF)** events originating in permafrost areas, which are documented on a catalogue.

In 2024, the PERMOS network included 27 field sites (Figure 1.1, Table 1.1). Ground surface temperature (GST) is measured at 22 sites at >200 locations. Ground temperatures are measured in 23 boreholes of 14–100 m depth at 14 sites. Six of these sites are equipped with automatic weather stations. Geophysical surveys are conducted annually along permanently installed profiles at 5 ground temperature sites. Rock glacier velocities are determined at 15 sites on 18 rock glaciers by annual terrestrial surveys. Eight rock glaciers are equipped with a permanent GNSS device for continuous measurements.

The selection of field sites for long-term permafrost observation followed a landform-based approach because permafrost change patterns related to topography, snow regime, and ground ice content are considered more important than those due to regional climate conditions (PERMOS 2019; Noetzli et al. 2024). Most of the PERMOS sites were installed in the framework of research projects and have been maintained by the partner institutions for several decades. The PERMOS monitoring strategy and sites are regularly evaluated and adapted based on relevance, technological advances, findings from research, and feasibility.

Seven partner institutions carry out instrument maintenance and data collection at the PERMOS sites: ETH Zurich, Universities of Fribourg (UniFR), Innsbruck (UIBK), Lausanne (UNIL) and Zurich (UZH), University of Applied Sciences and Arts of Southern Switzerland (SUPSI), and the WSL Institute for Snow and Avalanche Research SLF (SLF). The PERMOS Office, jointly run by SLF and UniFR, operates the network, implements the monitoring strategy, curates the data, and reports the results. PERMOS is financially supported by the Federal Office of Meteorology and Climatology MeteoSwiss in the framework of GCOS Switzerland, the Swiss Federal Office for the Environment (FOEN) and the Swiss Academy for Sciences (SCNAT). Two standing committees advise and supervise the activitites, from a political and financial point of view (PERMOS Steering Committee), as well as scientifically (PERMOS Scientific Committee).

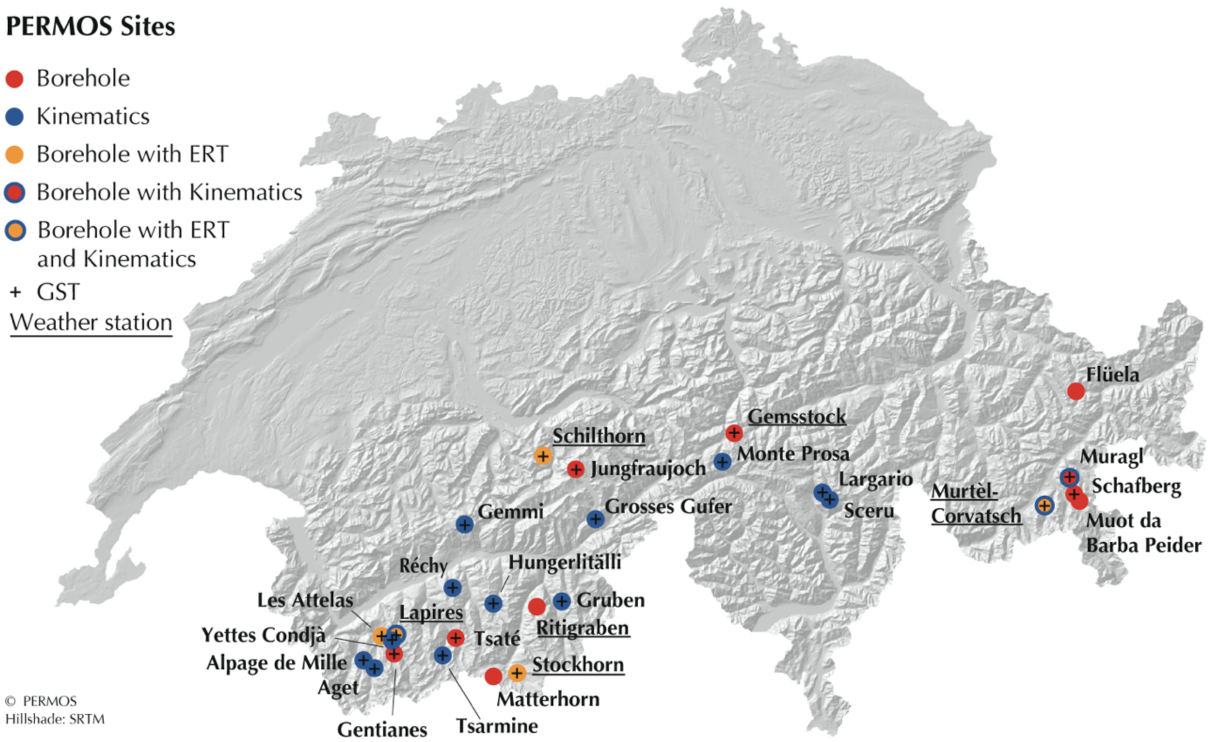

Figure 1.1. PERMOS field sites and measured variables.

Table 1.1. Location and characteristics of the PERMOS sites and type of variable measured at the site: BHT is borehole temperature (ground temperature measured in boreholes), GST is ground surface temperature, ERT is Electrical Resistivity Tomography, TGS is Terrestrial Geodetic Survey and GNSS are permanent GNSS devices. X and Y denote CH1903+ coordinates, and Z is the elevation in m asl. Coordinates indicate the general location of a site.

Name	Abb.	Region	Morphology	X	Y	Z	BHT	GST	ERT	TGS	GNSS	Meteo
Aget	AGE	Lower Valais	rock glacier	2584500	1095300	2800		X		X		
Les Attelas	ATT	Lower Valais	talus slope	2587200	1105000	2700	X	X	X			
Flüela	FLU	Engadine	talus slope, rock glacier	2791500	1180500	2400	X					
Gemsstock	GEM	Urner Alps	crest	2689800	1161800	2900	X	X				X
Gentianes	GEN	Lower Valais	moraine	2589400	1103600	2900	X	X				
Gemmi	GFU	Upper Valais	rock glacier, solifl. lobe	2614800	1139500	2750		X		X	X	
Grosses Gufer	GGU	Upper Valais	rock glacier	2649350	1141900	2400		X		X	X	
Gruben	GRU	Upper Valais	rock glacier	2640500	1113500	2800		X		X	X	
Hungerlitaelli	HUT	Upper Valais	rock glaciers	2621500	1115500	3000		X		X		
Jungfraujoch	JFJ	Bern. Oberland	crest	2641000	1155100	3700	X					
Lapires	LAP	Lower Valais	rock glacier, talus slope	2588070	1106080	2700	X	X	X	X		X
Stabbio di Largario	LAR	Ticino	rock glacier	2719000	1148500	2550		X		X	X	
Matterhorn	MAT	Upper Valais	crest	2618400	1092300	3200	X					
M. d Barba Peider	MBP	Engadine	talus slope	2791300	1152500	2950	X					
Alpage de Mille	MIL	Lower Valais	rock glacier	2581800	1096800	2500		X		X		
Monte Prosa	MPR	Ticino	rock glacier	2687450	1157700	2500		X		X	X	
Muragl	MUR	Engadine	rock glacier	2791000	1153700	2600	X	X		X	X	
Murtèl-Corvatsch	COR	Engadine	rock glacier, talus slope	2783150	1144700	2650	X	X	X	X	X	X
Réchy	REC	Lower Valais	rock glacier	2605900	1113300	3100		X		X	X	
Ritigraben	RIT	Upper Valais	rock glacier	2631700	1113700	2600	X					X
Schafberg	SBE	Engadine	rock glacier	2790900	1152700	2700	X	X				
Valle di Sceru	SCE	Ticino	rock glacier, talus slope	2720200	1145600	2500		X		X		
Schilthorn	SCH	Bern. Oberland	crest	2630400	1156400	2900	X	X	X			X
Stockhorn	STO	Upper Valais	crest	2629850	1092850	3400	X	X	X			X
Tsarmine	TMI	Lower Valais	rock glacier	2605300	1099400	2500		X		X		
Tsaté	TSA	Lower Valais	crest	2608500	1106400	3000	X	X				
Yettes Condjà	YET	Lower Valais	rock glacier	2588300	1105000	2700		X		X		

2 Weather and climate

Air temperature and snow depth are the most important meteorological variables that influence seasonal fluctuations and the long-term evolution of the thermal regime in the ground. Changes in air temperature drive temperature changes at the ground surface in periods with little or no snow, and all year round for locations where no thick winter snow cover can develop, for example in near-vertical bedrock slopes or on wind-blown ridges. The winter snow cover insulates the ground from the atmospheric conditions. The timing of the onset of snow cover in early winter and snowmelt in spring is therefore of great importance for the thermal regime in the permafrost: an early snow cover conserves the summer heat in the ground while a long-lasting snow cover insulates the ground from increasing air temperatures in early summer. Conversely, the ground can cool if the snow cover starts late at the beginning of winter or warm up earlier if the snow melts early in the spring. The weather and climate information given below is based on MeteoSwiss (2024, 2025) and Zweifel et al. (2024).

The hydrological year 2024 started in October 2023, in the second warmest autumn with air temperatures 2.2 °C above the mean of the recent long-term reference period 1991–2020. October 2023 was the second warmest October since the start of the measurements in 1864 (Figure 2.1). The very warm autumn was followed by an early start of winter snow fall at high elevations. From mid-November to Christmas 2023, snow fell repeatedly north of the main Alpine ridge leading to snow depths well above average at high-elevation stations (Figure 2.2). During winter 2024, a dry period was only experienced from the end of January to the beginning of February. From February to April 2024, large amounts of snow fell on the southern slopes of the Alps. Overall, the winter 2024 was one of the warmest and wettest on record, with above-average snow depths first along the main Alpine ridge and from mid-winter onwards in the Southern Alps. Except for November 2023, every month of the winter half-year was warmer than the average of the 1991–2020 reference period. February 2024 was even the warmest ever recorded with 4.6 °C above the 1991–2020 mean (Figure 2.1).

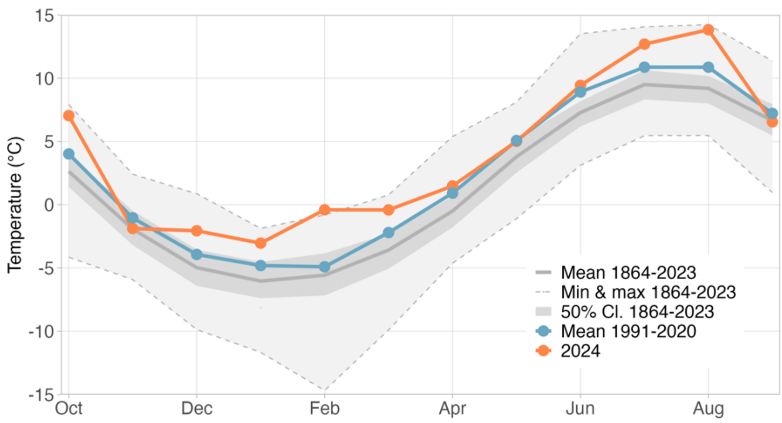

Figure 2.1. Monthly mean air temperatures of the hydrological year 2024 (October 2023 to September 2024) compared to previous measurements since 1864 and the mean of the most recent reference period 1991–2020. Data source: MeteoSwiss, homogenized data series for Swiss stations above 1000 m asl.

Spring 2024 was rather wet and mild, with air temperature 0.8 °C above the average 1991–2020 and with below-average sunshine duration. Subsequently, Switzerland experienced the sixth warmest summer on record, staring with a very warm July. Local temperature records were registered in August, which was very sunny and the second warmest August recorded since 1864 (Figure 2.1). At the high elevation stations Weissfluhjoch or Säntis, August 2024 was even the warmest month on record. The amount of precipitation during summer 2024 was mostly below average. The hydrological year 2024 ended with an averagely warm September 2024 and with a temperature drop and first snow fall at high elevations in the first half of the month.

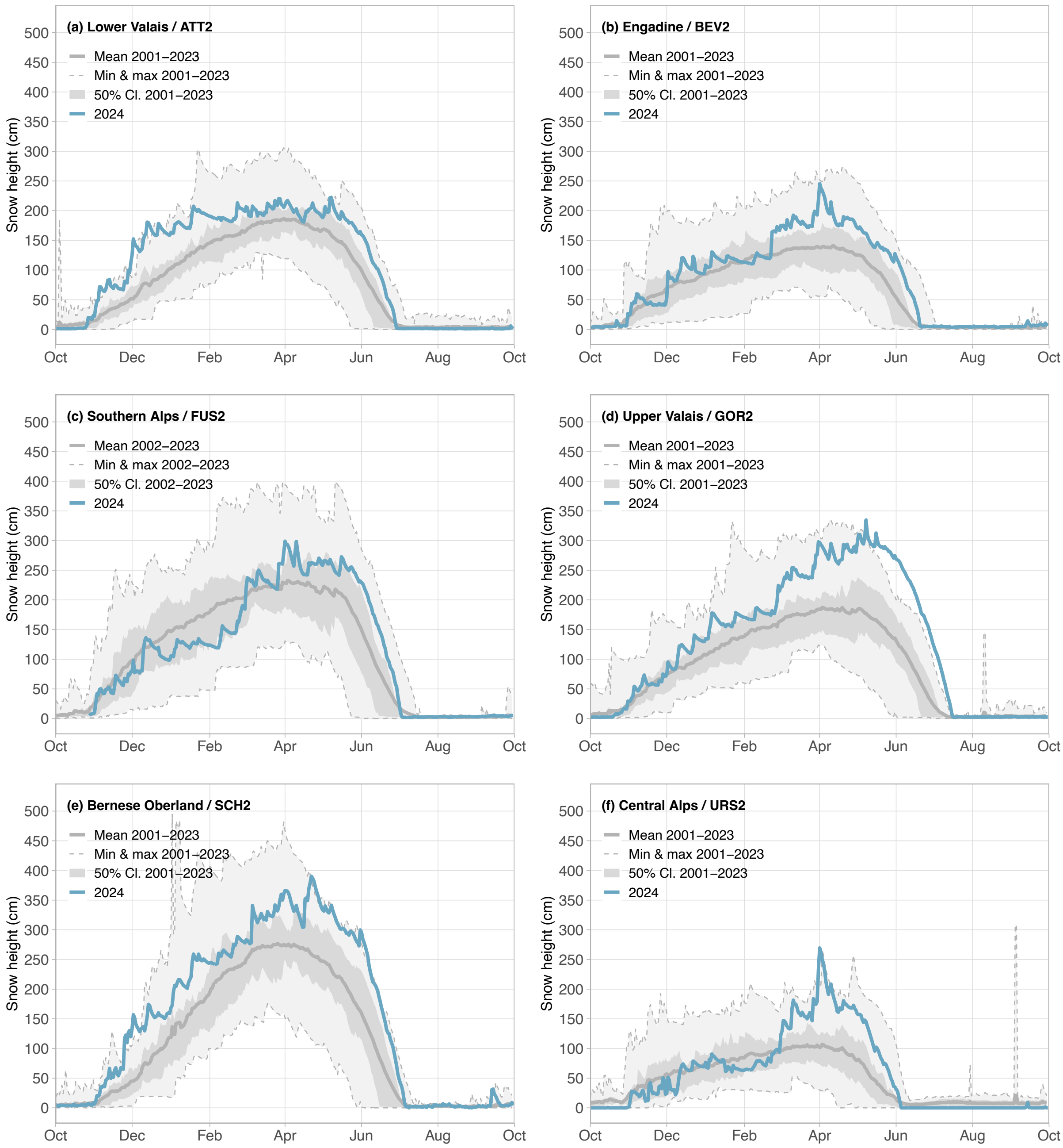

Figure 2.2. Snow height at six IMIS weather stations during winter 2024 compared to the mean, 25th and 75th percentiles of the period 2001–2023. Data were corrected for outliers and aggregated to daily median values. The stations represent different regions in the Swiss Alps: a) Lower Valais, b) Engadine, c) Southern Alps, d) Upper Valais, e) Bernese Oberland, and f) Central Alps. Data source: IMIS/SLF.

In summary, the hydrological year 2024 was characterized by a very mild and snow-rich winter, a cool and wet spring, and very warm atmospheric conditions in summer and autumn 2024. It was the second warmest hydrological year in Switzerland above 1000 m asl. since the start of the measurements in 1864 (the calendar year 2024 was the third warmest year) (Figure 2.3). The mean annual air temperature (MAAT) was 2.65 °C above the 30-year average 1961–1990 (the reference period for long-term monitoring of climate change by WMO) (Figure 2.3) and 1.44 °C above the most recent reference period 1991–2020.

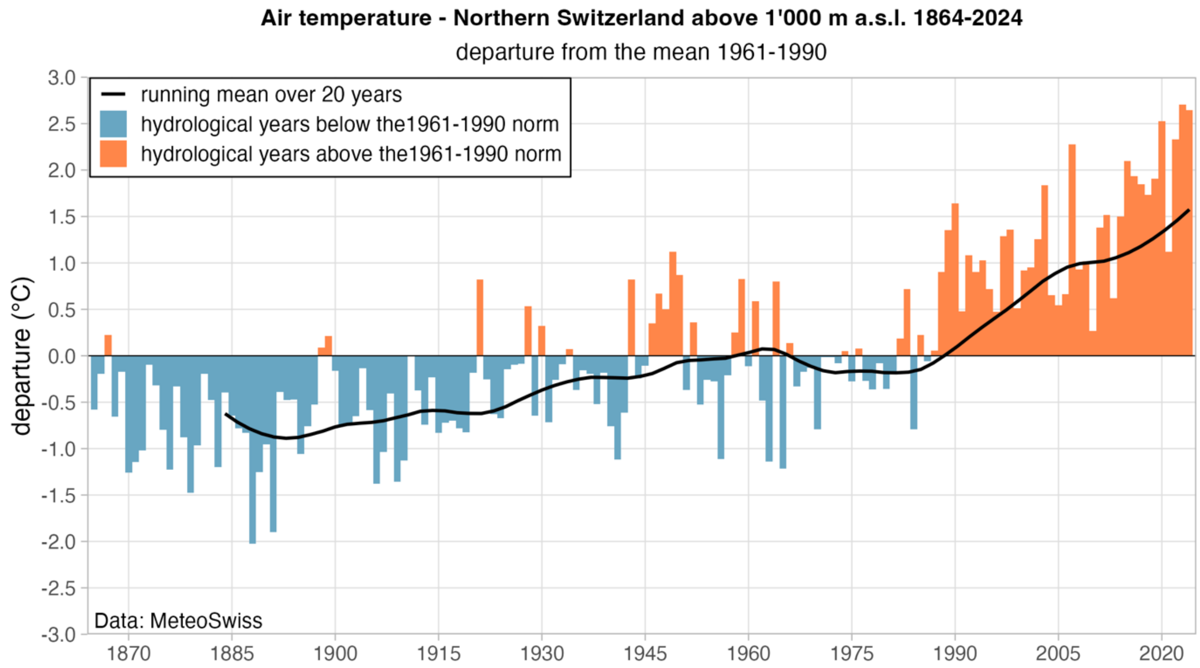

Figure 2.3. Air temperature deviation from the 1961–1990 climate norm based on homogenized data series for Swiss stations above 1000 m asl. for 1864–2024. Annual values refer to the hydrological year (October to September). Adapted from MeteoSwiss, data source: MeteoSwiss.

3 Ground temperatures and active layer thickness

Ground temperatures are the direct, quantitative, and comparable observations of the permafrost thermal state. They are continuously measured at multiple depths in boreholes (Section 3.3). The point information obtained from these observations is complemented by spatially distributed measurements of the ground surface temperature (obtained at approximately 10 cm depth, Section 3.1). Continuous ground temperature measurements in permafrost are also used to derive the active layer thickness (ALT, i.e., the maximum thickness of the topmost ground layer that thaws annually during summer) (Section 3.2).

3.1 Ground surface temperatures

Ground surface temperature (GST) observations capture the thermal conditions at the ground surface. They subsequently penetrate deeper into the ground with increasing delay and attenuation. Spatially distributed measurements allow the assessment of spatial variability related to varying topographic settings or ground surface characteristics. GST results from the energy balance at the ground surface, which is predominantly influenced by solar radiation and air temperature during snow-free periods (e.g., Hoelzle et al. 2022). During the snow season, the ground surface is insulated from atmospheric conditions. The timing of the snow cover therefore impacts GST, except for locations where a thick winter snow cover cannot develop, such as in steep rock walls or on wind-blown ridges.

GST are recorded with miniature temperature data loggers, which are distributed close to boreholes, along geophysical profiles and next to geodetic survey points. Loggers are buried at around 10 cm depth to shield them from direct solar radiation, which would cause warming of the casing. Recording intervals are 1–3 hours, depending on the storage capacity of the device used.

For reporting in this bulletin, individual GST time series were aggregated to daily mean values and gap-filled applying the quantile mapping approach described by Staub et al. (2017). We then selected the time series that cover at least five years as well as the reporting period and have values for 85% of the time after gap filling. To aggregate the daily temperatures to monthly and annual mean values, we apply the data completeness criteria defined for air temperatures by WMO (2017). Site means are calculated for periods where data are available for all selected GST time series at a site. That way, the PERMOS GST data set 2024 includes 19 sites with 2–9 time series per site. In total there are 84 time series. Data from 2 sites only cover summer 2024, but not September (GFU and LAP) and are only included for analyses of the winter conditions.

The mean annual ground surface temperature (MAGST) in the hydrological year 2024 was above the decadal mean 2012–2021 for 15 of 17 sites (88%). At six of the sites a new maximum MAGST was recorded since the start of the measurements. For all sites but two, the MAGST 2024 was among the four warmest measured so far. The running annual mean of the daily GST (rMAGST, Figure 3.1b, Figure 3.2b, Figure 3.3) strongly increased during the first half of the hydrological year 2024 and reached a new maximum between April and June 2024 for most of the sites (13 of 19 sites, 68%). This is mainly the result of high and often record temperatures at the ground surface during winter 2024 (Figures 3.1a and 3.2a), which were caused by the early snow fall on very warm ground in autumn 2023 (see Section 2). After the peak in spring 2024 the rMAGST decreased due to a mild spring and early summer but remained at or close to record level. At all monitored sites, the maximum rMAGST was observed in the past 5 years and surpassed previous record values registered after the summer heat waves in 2003 or 2015. When considering a running mean value over two years (rM2AGST), new record values were reached in 2024 for 17 of the 19 sites (89%). This points to the cumulative effect of two very warm years.

For the seven sites with the longest GST time series (i.e., starting in the year 2000 or before) a warming rate of 0.4–0.8 °C dec^{-1} is calculated based on linear regression on MAGST over a 25-year period 2000–2024 (sites AGE, GFU, LAP, MIL, REC, SCH, YET).

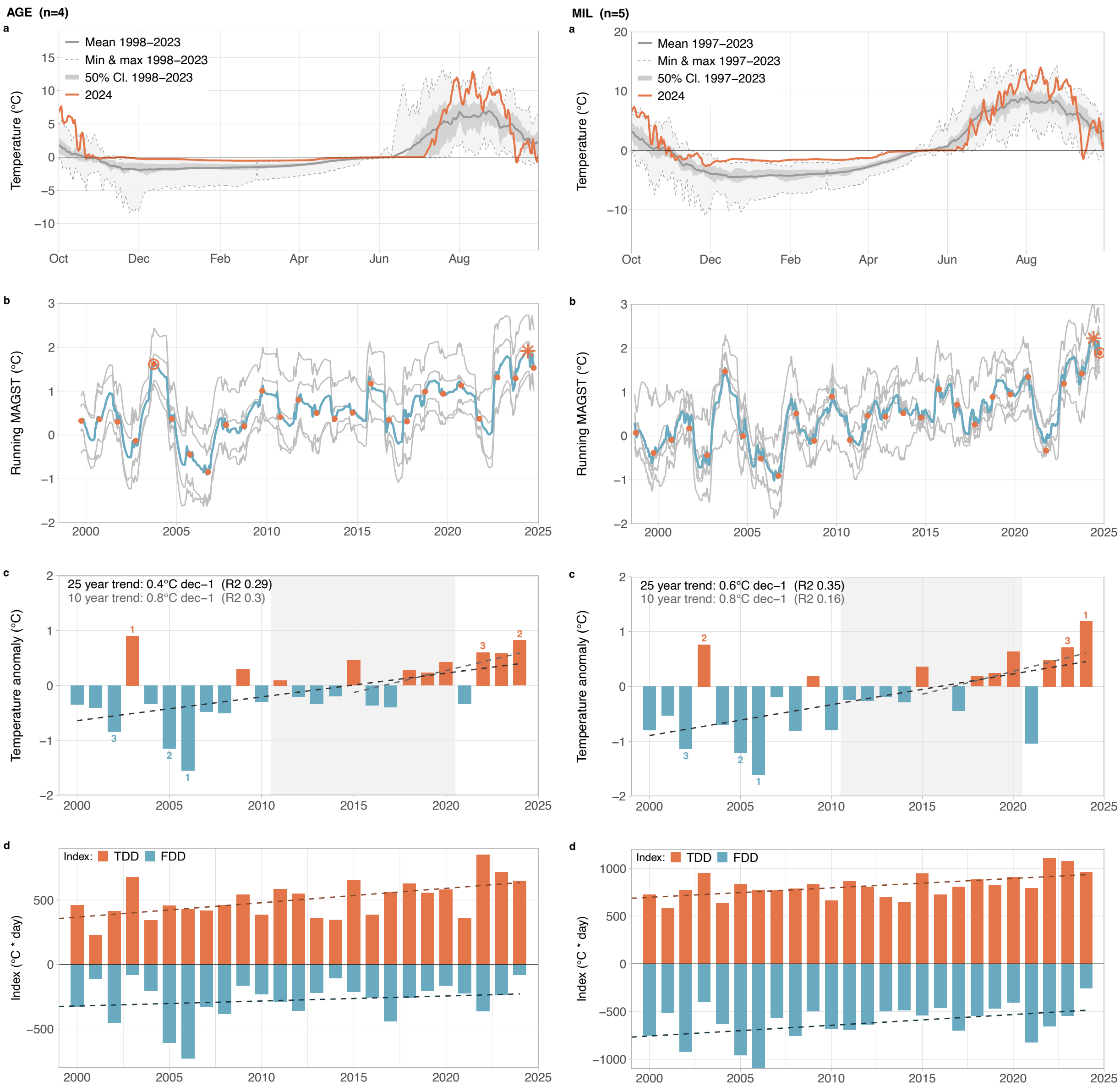

Figure 3.1. Ground surface temperatures at two rock glacier sites in the Lower Valais with long and complete time series: Aget (AGE, left) and Réchy/Bec de Bosson (REC, right). a) Daily mean GST at the sites during the hydrological year 2024 compared to all previous years. b) Running annual mean for the site mean (rMAGST, thick blue line) and all individual loggers in grey. Mean annual ground surface temperature (MAGST) is shown with orange dots. The maximum MAGST is marked with a circle, the maximum rMAGST with an asterisk. c) Departure of the MAGST from the 2012–2021 decadal mean. Trends for the last one and two decades are shown with dashed lines. d) Ground thawing and freezing indexes.

The Ground Freezing Index (GFI) is defined as the sum of the negative daily temperatures during a hydrological year and is an indication of how cold a winter season was. GFI in 2024 is higher (i.e. less negative) than in the previous year and the highest recorded for more than half of the sites (i.e., the smallest negative number) (Figures 3.2d and 3.3d, blue bars). This points again to the warm conditions during winter 2024. The Ground Thawing Index (GTI) is defined as the annual sum of positive daily temperatures and is an indication of how warm the thawing season was. It can only be determined for sites with data extending to the end of the hydrological year. GTI values are lower in 2024 than in the previous summer, reflecting the mild spring and lower summer temperatures in 2024 compared to 2023 (Figures 3.1d and 3.2d, orange bars).

Figure 3.2. The same as figure 3.1, but flat bedrock with winter snow cover (COR_R, left) and near-vertical bedrock without winter snow cover (COR_W, right) in the Corvatsch area in the Upper Engadine.

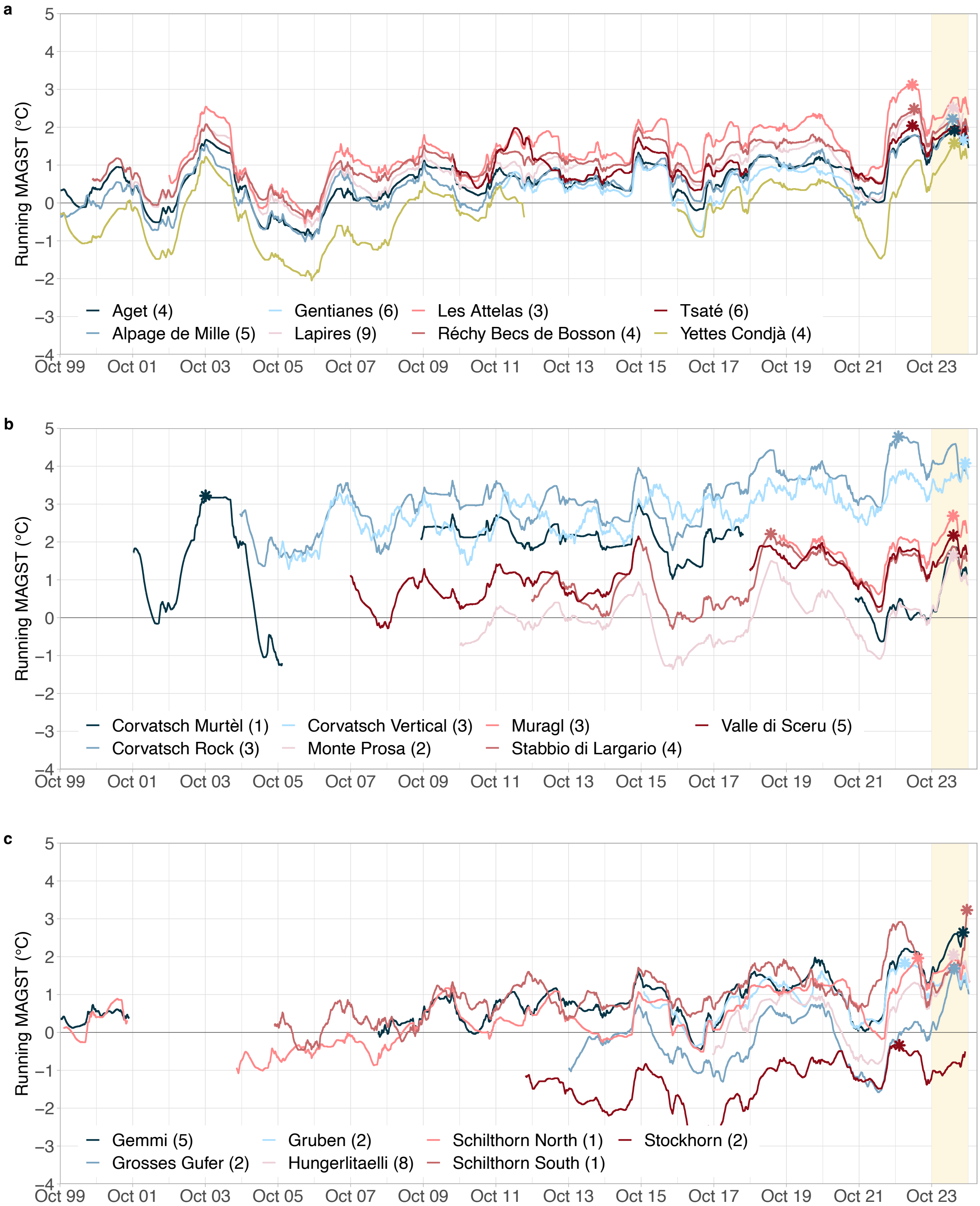

Figure 3.3. Running mean annual ground surface temperature (rMAGST) for sites in (a) the Lower Valais, (b) the eastern and Southern Swiss Alps, and (c) the Upper Valais, central and Northern Swiss Alps. The maximum value of rMAGST is indicated with an asterisk. The reporting period is highlighted with a yellow background. Corvatsch Rock, Corvatsch Vertical and Gemsstock are measured in flat and near-vertical bedrock, all other sites are in unconsolidated material (rock glaciers and talus slopes). Series depict site averages of several individual time series (cf. number of loggers in brackets).

3.2 Active layer thickness

The Active Layer Thickness (ALT) is defined as the maximum penetration depth of the 0 °C isotherm during summer and autumn. The base of the ALT is the permafrost table, and the actual permafrost body lies below. The inter-annual variations of the ALT are influenced by thermal conditions at the ground surface and in the uppermost metres during the hydrological year, as well as by the ground ice content. In ice-rich ground they are considerably smaller than in ice-poor bedrock because of latent heat effects (i.e., the energy exchanged during phase change). The latter dampens inter-annual fluctuations as it absorbs a considerable proportion of the additional energy in a warm year.

The ALT is calculated by linear interpolation of daily ground temperatures measured at two depths in boreholes, using the lowermost sensor in the active layer (T>0 °C) and the uppermost sensor in the permafrost (T≤0 °C). Because freeze/thaw processes and varying ground characteristics in the uppermost meters result in a non-linear temperature profile, changes in ALT must be interpreted with care, particularly in ice-rich ground. The direction of the trends and the magnitude of the variations are nevertheless considered robust.

Table 3.1. Active layer thickness (ALT) at the end of 2024 and corresponding date for PERMOS boreholes. The difference to the ALT in the previous year 2023 is given as well as the year with the maximum ALT. All ALT values are in metres. Values in italics are intermediate values because the available data does not yet cover the entire thawing period. Boreholes in which only an approximate range of the ALT can be determined, typically due to broken or unreliable sensors at the relevant depths or due to gaps in the time series, are also listed. Boreholes in which no ALT can be determined are not listed.

Borehole	ALT 2024	Date	Diff. 2023	First year	Max year	Comment
Attelas 0108	*5.0*	2024-08-31	0.1	2009	2024	Available data ends 2024-10-04
Attelas 0208	*6.0*	2024-09-05	0.1	2009	2024	Available data ends 2024-10-04
Murtèl-Corvatsch 0315	4.5	2024-08-14	<0.1	2016	2024	New time series since 2015
Gentianes 0102	–	–	–	2003	–	ALT between 5.09 and 9.57
Gentianes 0222	4.1	2024-09-26	0.1	2023	2024	
Lapires 0198	6.7	2024-09-10	<0.1	1999	2024	
Lapires 1208	7.31	2024-10-31	1.6	2010	2024	
Muot da Barba P. 0296	–	–	–	1997	–	ALT < 4.6 m, no sensor left in ALT
Muot da Barba P. 0319	3.2	2024-09-15	0.2	2020	2024	
Muragl 0424	*4.9*	2024-09-27	–	2024	–	New, drilled in August 2024
Ritigrabe 0102	5.6	2024-09-12	0.3	2002	2024	Thermistor at 4 m may be inconsistent
Schafberg 0190	*5.4*	2024-09-10	0.3	2005	2024	Available data ends 2024-09-11
Schafberg 0290	*5.2*	2024-09-11	<0.1	1997	2024	Available data ends 2024-09-11
Schilthorn 5198	–	–	–	1998	2022	No ALT after 2022, thaw depth ca. 13 m
Schilthorn 5200	–	–	–	2001	2017	No ALT after 2017, thaw depth ca. 15 m
Schilthorn 5318	–	–	–	2019	2021	No ALT after 2021, thaw depth ca. 15 m
Stockhorn 6000	*5.2*	2024-09-11	<0.1	2001	2024	
Stockhorn 6100	5.8	2024-09-24	0.5	2001	2024	

The ALT for the year 2024 could be determined for 13 of 23 boreholes at 9 sites (Table 3.1, Figure 3.4). For 4 of these boreholes the calculated ALT is an intermediate value because the time series does not yet extend to the end of the thawing period and the ALT may be larger (ATT_0108, ATT_0208, SBE_0190, SBE_0290). For two boreholes, only an approximate range of ALT can be given due to defective sensors at the respective depths (GEN_0102, MBP_0296). For the three boreholes on Schilthorn, ALT can no longer be determined because the active layer did not completely refreeze in winter (only the uppermost part). Here, only the thaw depth can be indicated, which is the thickness of the unfrozen layer above the remaining permafrost body.

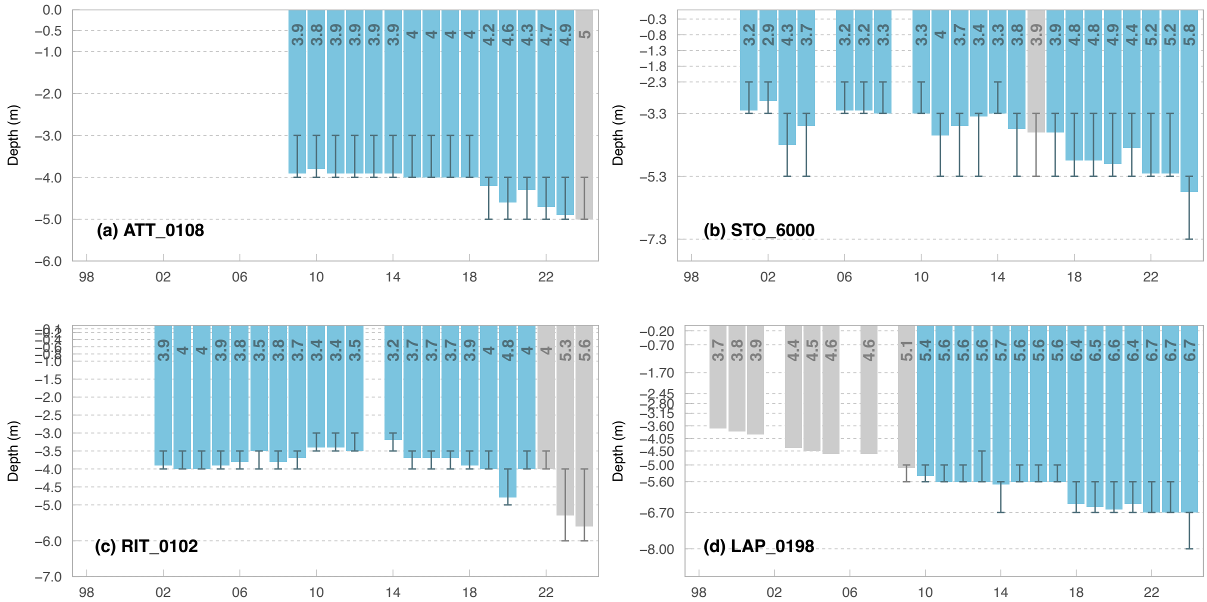

Figure 3.4. Active layer thickness (ALT) derived from ground temperature time series measured in the Attelas talus slope (a), on the Stockhorn plateau (b), in the Ritigrabe rock glacier (c), and in the Lapires talus slope (d). The uncertainty bars are defined by the thermistors used for the interpolation of the ALT (thermistor above and below 0 °C). Grey colours indicate an estimated ALT due to questionable data quality (e.g. in case a sensor is not fully reliable) or when the available data does not cover the entire thawing period 2024.

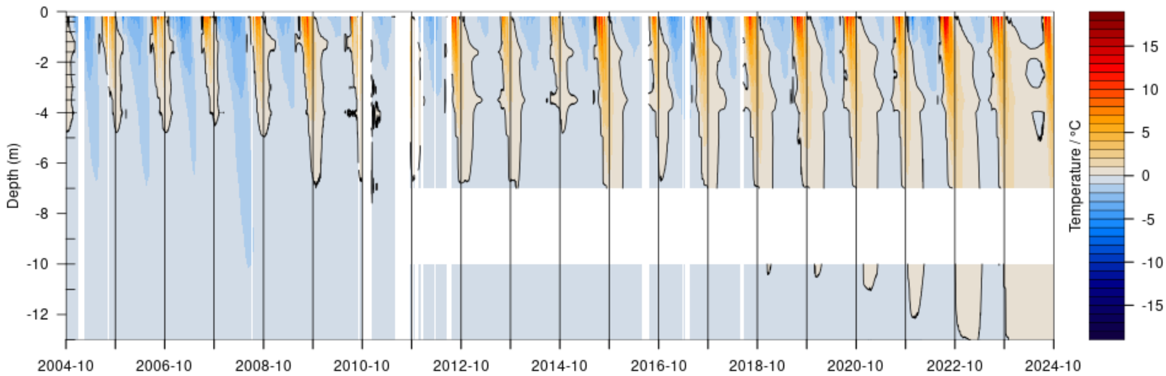

Figure 3.5. Permafrost temperature evolution at the Schilthorn in the Bernses Alps in borehole SCH_5198 in the past 20 years. Here the active layer did not refreeze in winter and permafrost only remains below a depth of about 15 m (this information is taken from two boreholes close by reaching to larger depth).

In one borehole, no ALT value is available because the data does not extend to the thawing period 2024 (MAT_0205). In four boreholes, the calculation of ALT is not possible because there is no permafrost (MUR_0199, GEM_0106) or because there are no (more) or possibly erroneous sensors at the relevant depths (MUR_0499, JFR_0195, LAP_1108, TSA_117).

ALT values calculated for the hydrological year 2024 were between 3.2 m (MBP_0319) and 7.3 m (LAP_1208). All ALT values available for 2024 were larger than the previous record values observed (Table 3.1, Figure 3.4). A talik formed at Schilthorn at 2900 m asl., which can be observed in all three active boreholes (Figure 3.5). The thaw depth is about 15 m and permafrost only remains below this depth. This is a clear sign of permafrost degradation.

3.3 Permafrost temperatures

Ground temperature variations are primarily driven by changes in the ground surface temperature (GST, Section 3.1), which follow the meteorological conditions in the snow-free period (Section 2). In the uppermost metres below the surface, ground temperatures react to short-term variations in GST. These variations are increasingly dampened and delayed with depth. At 10 m depth, only larger seasonal variations are reflected, with a delay of about half a year. At the so-called depth of the zero annual amplitude (DZAA), seasonal variations are below 0.1 °C. The DZAA is typically at 15–20 m in permafrost in the Swiss Alps. Below, ground temperatures react to multi-annual changes from atmospheric conditions with delays of years (around 20 m depth) to decades (> ca. 50 m depth).

Continuous permafrost temperatures are recorded at multiple depths in 23 boreholes at 14 sites (Table 1.1). All boreholes are instrumented with multi-sensor cables and automatic logging systems. Many of them are equipped with data transmission systems, while for others the data is collected on site once a year during the field work season. For the latter, the available data often do not yet cover the entire hydrological year until October 2024 because field work typically takes place earlier. The recording interval varies between 1 and 24 h depending on the instrumentation. The observations follow the guidelines for long-term borehole temperature measurements (Noetzli et al. 2021, Streletskiy et al. 2021, WMO 2024). Permafrost temperature data are quality-checked for outliers. Further inconsistencies such as noise, jumps or sensor drift are detected based on visual inspection and plausibility (i.e., consistency with neighbouring data). The time series are subsequently aggregated to daily, monthly, and annual mean values using depth-dependent criteria for data completeness (cf. also Noetzli et al. 2024).

Figure 3.6. Drilling of a new borehole for permafrost temperature measurements on rock glacier Muragl in the Upper Engadine in August 2024. Photo: J. Noetzli.

Several challenges and changes to the PERMOS borehole network occurred in the past 2 years, which are related to the age of the instruments and/or to changing conditions at the observation sites. The borehole in the Flüela talus slope (FLU_0102) is not accessible for safety reasons (rock fall). Borehole MBP_0196 at Muot da Barba Peider above Pontresina no longer records data due to sensor failure. Two of three active boreholes on rock glacier Murtèl-Corvatsch were destroyed by a rock fall in September 2023, and the related temperature time series cannot be continued (COR_0287 and COR_0200). The borehole drilled in the year 2015 to ensure the continuation of the longest continues time series in mountain permafrost (COR_0315) could be repaired and is operating. On rock glacier Muragl above Samedan (GR), a new 15 m deep borehole was drilled in August 2024 (MUR_0424) to continue ground temperature measurements at the site (Figure 3.6). The three previous boreholes in permafrost were sheared off due to the rock glacier movement and do no longer deliver data. One active borehole next to the rock glacier is not in permafrost (MUR_0199).

During the hydrological year 2024, the mean annual permafrost temperatures at 10 m depth increased compared to 2023 in all 16 PERMOS boreholes, with data covering the entire reporting period (Figure 3.7). In six boreholes, the increase is ca. +0.2 °C, at eight boreholes the increase is in the order of +0.1 °C, and at three boreholes the increase is <+0.1 °C. These three are in ice-rich, warm permafrost (ATT_0208, GEN_0102, SBE_0190). In 14 boreholes (88%), the mean temperature of the hydrological year 2024 at 10 m depth was higher than previously measured and mark a new maximum. The considerable warming in 2024 was to a large part driven by exceptionally high winter temperatures at the ground surface (Figure 3.8, note: the lowest values of the annual temperature wave at 10 m depth are typically observed with several months delay compared to the surface temperatures, i.e. during the summer months).

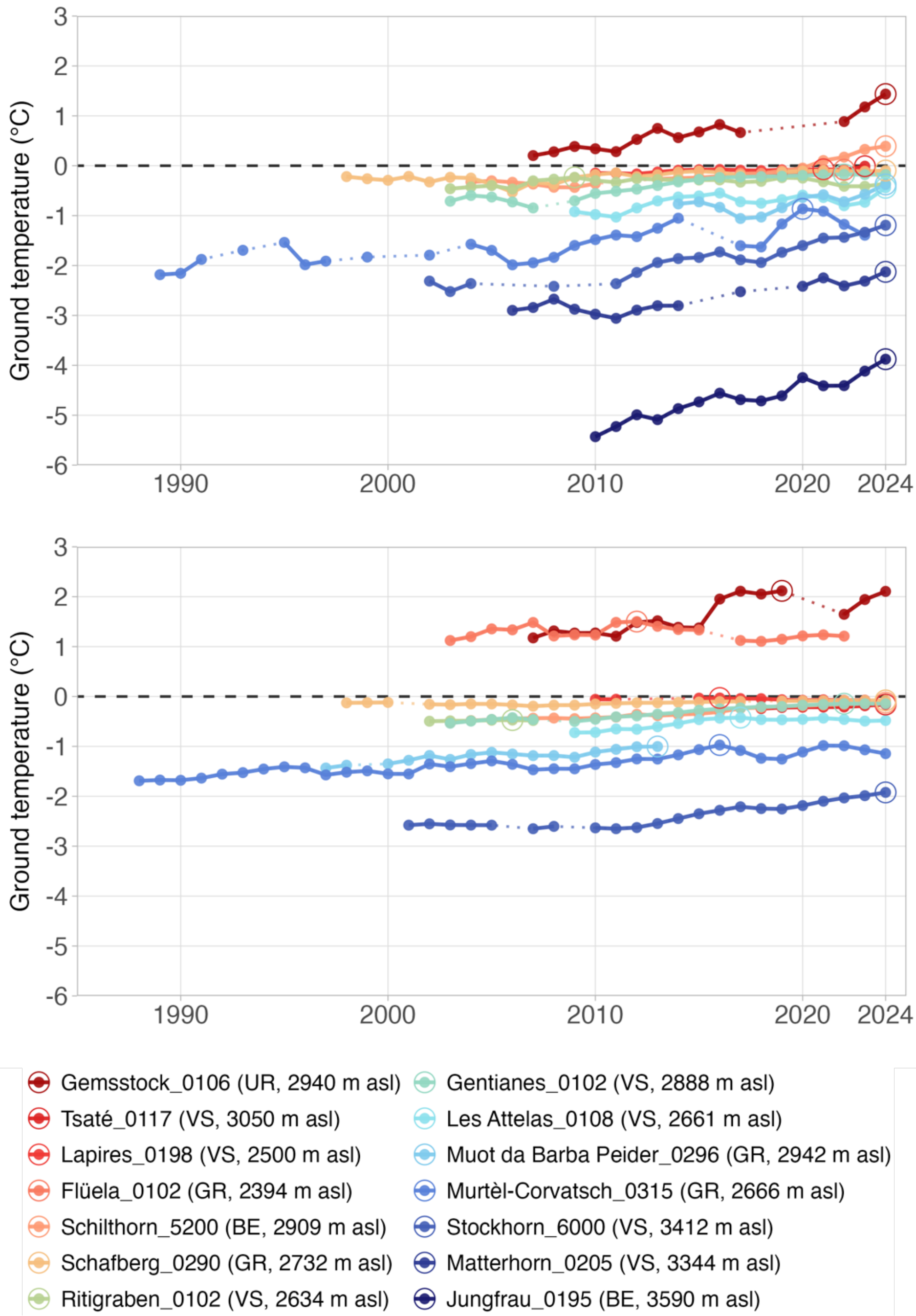

Figure 3.7. Ground temperatures measured in selected PERMOS boreholes at 10 m (top) and 20 m depth (bottom). The temperatures are shown as mean values for hydrological years. Maximum values for each time series are shown with circles.

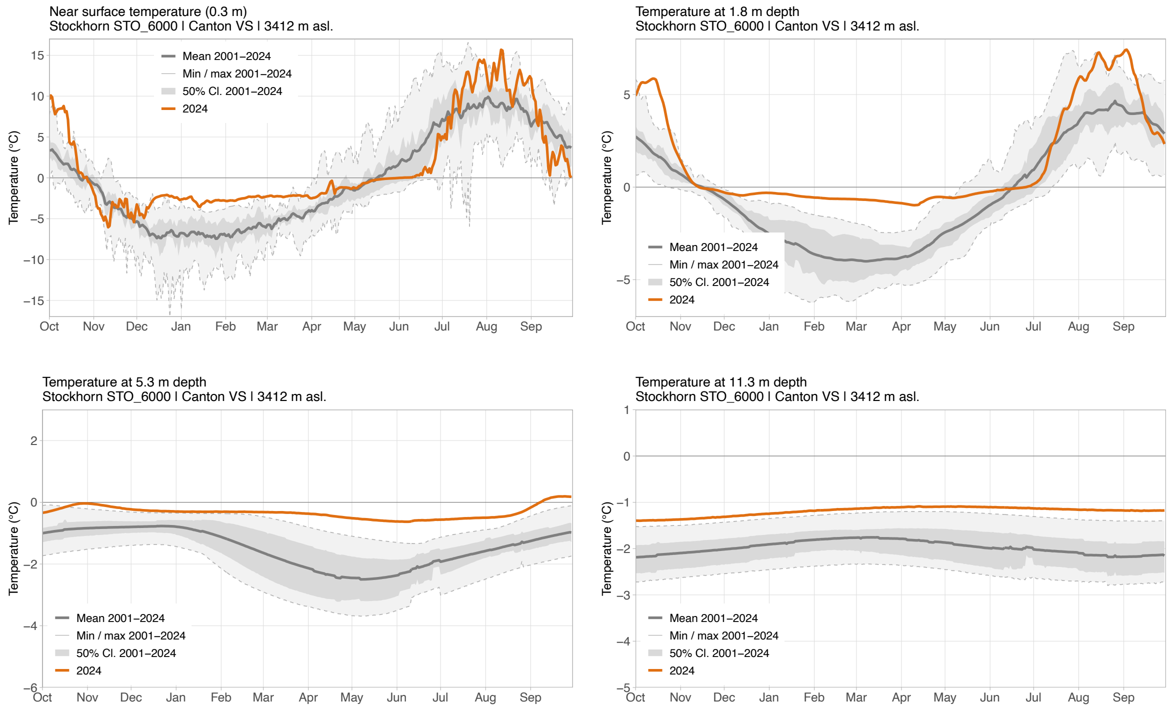

Figure 3.8. Evolution of daily ground temperatures during the hydrological year 2024 at different depths in the uppermost 10 m of the borehole on Stockhorn above Zermatt at 3400 m asl. (STO_6000). The ground temperatures measured in the hydrological year 2024 are shown in orange and compared to all previous measurements in the borehole starting in the year 2001. Panels show the annual temperature evolution close to the surface (upper left), at ca. 2 m depth (upper right), at ca. 5 m depth (lower left), and ca. 10 m depth (lower right).

At 20 m depth, temperatures react with more delay to changes in GST. Here, the permafrost temperatures increased in 11 of 15 boreholes in 2024 compared to the previous year and by a smaller amount (mostly 0.02–0.1 °C). In four boreholes a slight decrease of 0.07 °C or less was recorded at 20 m depth. At 20 m depth, in 50% of the boreholes with data available until October 2024 several new record values were observed in the hydrological year 2024.

On a decadal perspective, ground temperatures have increased at Swiss borehole sites in permafrost areas up to 1.1 °C at 10 m depth in the last decade 2015–2024, with a mean of 0.4 °C (see Noetzli et al. 2025). A lower mean change rate of 0.2 °C per decade was observed at 20 m depth, which results from the increasing delay in the temperature signal penetrating at depth. The highest change rates are observed at ice-poor and cold bedrock locations (ca. 0.6 °C dec^{-1}), whereas very low change rates are observed at ice-rich sites with temperatures only just below 0 °C. Here, warming rates are reduced because ice melt requires energy for phase change. In warm permafrost (>–2 °C) with a high ground ice content, temperature changes are reduced because of latent heat exchange during phase change (Noetzli et al. 2024, 2025). Just below 0 °C temperature changes become minimal and can remain nearly stable for many years. The warming rates and change patterns are congruent with values observed in European mountain regions (Noetzli et al. 2024).

To detect changes in warm or near-zero permafrost, additional measurements sensitive to changes in ground ice and liquid water content are needed to observe changes in the permafrost until the frozen material has thawed entirely (see Section 4).

4 Electrical resistivities of permafrost

Electrical Resistivity Tomography (ERT) exploits the different electrical properties of the subsurface components. This method is particularly sensitive to the presence of liquid water in the subsurface and is therefore well suited to distinguish frozen from unfrozen terrain. By repeating ERT surveys with an identical measurement setup (profile location and geometry), changes in the subsurface properties and more specifically changes in liquid water and ice content in the ground can be observed, which cannot be detected with the thermal measurements described above. In a permafrost environment, decreasing electrical resistivities indicate an increase of the ratio between liquid water and ice content, and may point to an overall ground ice melt. Conversely, increasing electrical resistivities can be caused by an increase of the ground ice content and/or a decrease in liquid water content, but they may also indicate an overall drying of previously wet conditions, e. g. in the active layer.

Within the PERMOS network, electrical resistivities are measured at five sites along profile lines between 96 and 235 m length. The ERT monitoring installations include 43 to 50 permanently installed electrodes (stainless steel rods), which are connected by cables to a box, to which the measurement device can be connected (see Figure 4.1). Measurements are performed annually at the end of summer (end of August to October). Measured resistivities are quality controlled and inverted following the procedure described in Mollaret et al. (2019).

Figure 4.1. Electrical Resistivity Tomography (ERT) monitoring installation at Murtèl-Corvatsch. Photo: C. Pellet.

The electrical resistivities measured at the five PERMOS sites span several orders of magnitude due to the site specific different sub-surface characteristics (i.e. ice-content, sub-surface type) (Figure 4.2). The lowest values are obtained at Schilthorn (~1’500 Ωm), an ice-poor bedrock site with permafrost temperatures close to 0 °C. The highest resistivities are measured at Murtèl-Corvatsch (~200’000 Ωm), a rock glacier site characterized by a coarse blocky surface and an ice rich core.

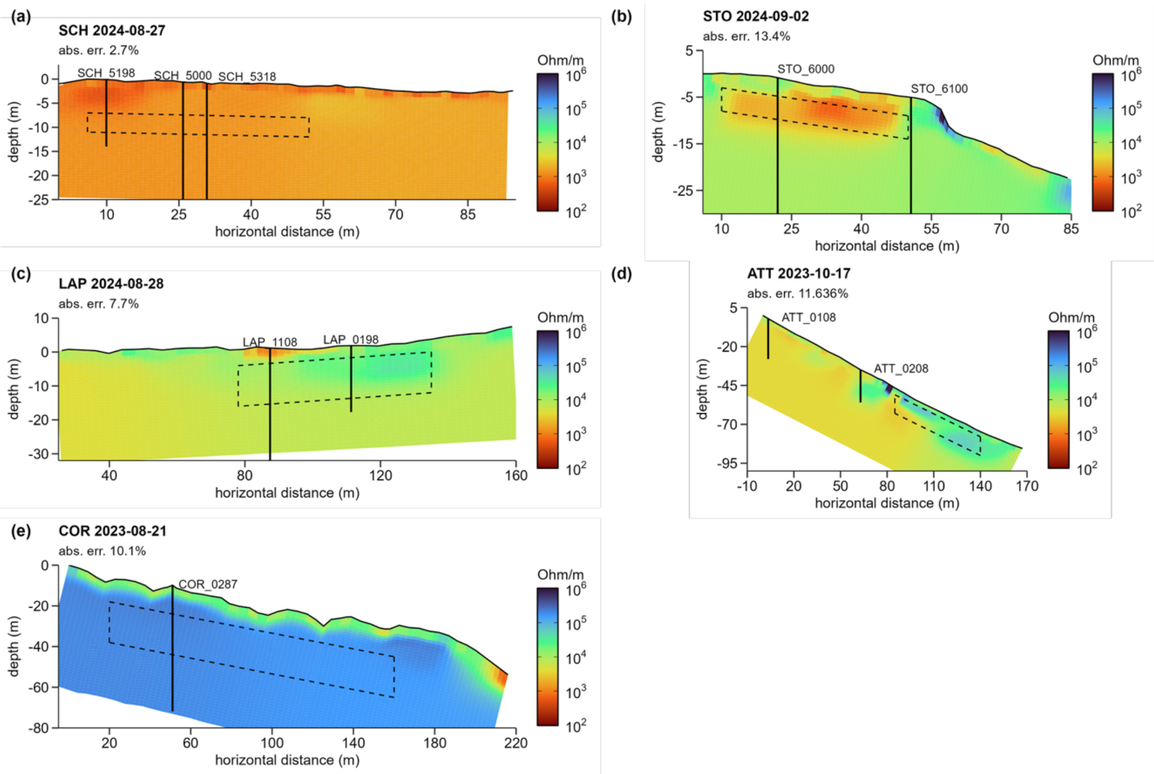

Figure 4.2. Electrical Resistivity Tomograms showing the resistivity distribution at two bedrock sites (Schilthorn, a and Stockhorn, b), two talus slopes (Lapires, c and Les Attelas, d) and one rock glacier (Murtèl-Corvatsch e) in 2024 (a–c) and 2023 (d–e). The representative zones used to derive the time series in Figure 4.3 are indicated with dashed boxes and the borehole locations are shown with vertical black lines.

Spatially averaged resistivity values are computed for manually selected zones within the ERT tomograms to perform inter-site comparison and analyse the temporal evolution (Figure 4.2). These zones are delineated to encompass the largest possible homogeneous part of the permafrost (based on temperature and resistivity) and the part of the tomogram with the highest measurement sensitivity and quality (i.e. excluding the lateral and deep edges of the tomogram). The active layer is excluded wherever possible to focus on the permafrost and zones subject to longer-term variations. Since 2024 at Schilthorn, the representative zone no longer is in permafrost conditions due to the formation of a talik (see Figure 3.5).

Since the start of the observations, resistivities measured within the permafrost layer generally decreased at all sites (Figure 4.3). This trend is consistent with the reported increase in ALT and permafrost temperatures. It indicates a general increase in liquid water content within the permafrost, which is considered a direct consequence of ground ice degradation and enhanced infiltration of water.

ERT surveys were performed at three sites in 2024. No field work was possible at Murtèl-Corvatsch and Les Attelas due to safety issues caused by rockfall activity. The data quality was satisfactory for the measured profiles (see Mollaret et al. 2019 for detailed description of the quality assessment and threshold). At Stockhorn, resistivities within the representative zone decreased by –20% compared to 2023 and by –31% compared to 2022. At Lapires, the resistivity decreased by –7% compared to 2023. At Schilthorn, the average resistivity increased by +5% compared to 2022.

Stockhorn is a bedrock site with comparatively low ice content, where ground temperatures are mostly controlled by conductive heat transport, thus explaining the observed decrease. The large resistivity decrease is in line with the record ALT and permafrost temperatures observed in 2024. Lapires is a coarse blocky site with higher ice content, where conductive heat transport occurs in addition to latent heat exchange and heat convection/advection via ventilation within the coarse blocky material. The comparatively smaller resistivity decrease is in line with the smaller ALT and permafrost temperature increase reported in 2024. Schilthorn is a bedrock site with previously extremely low ice content and permafrost temperatures very close to 0 °C. The ice has now disappeared within the representative zone and the temperatures remained above 0°C throughout the entire hydrological year 2024 (see Figure 3.5). Increasing resistivities observed in 2024 could indicate that the thaw layer, which did not refreeze during the winter 2024, is now drying.

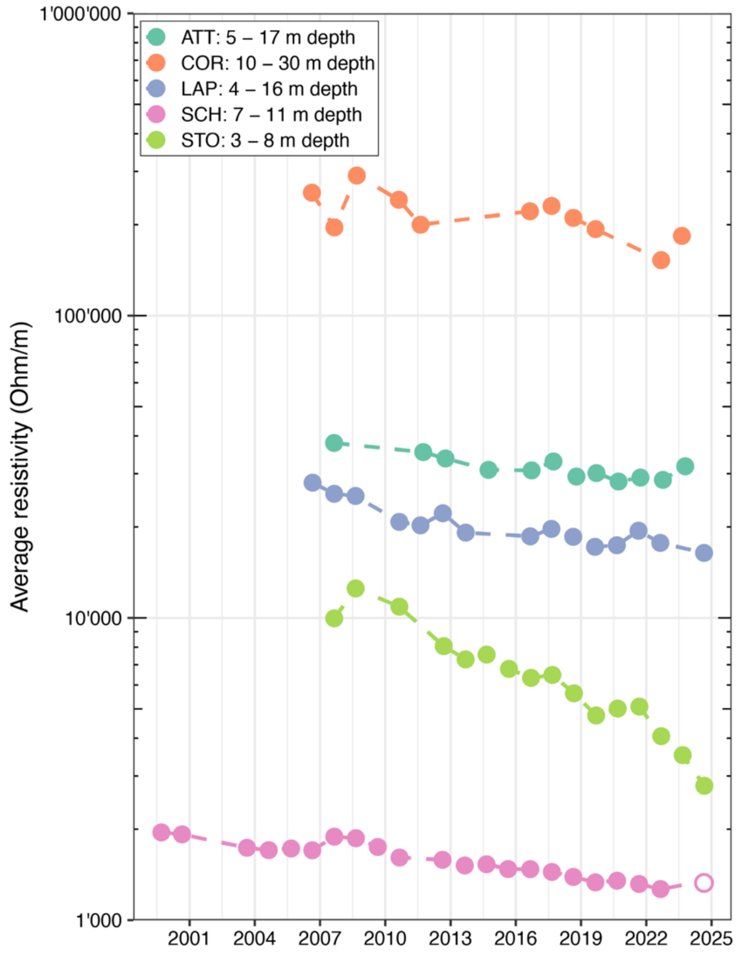

Figure 4.3. Average electrical resistivities of the representative zones (see Figure 4.2) at the end of summer for the 5 ERT sites in the PERMOS Network. Note that at Schilthorn in 2024, the representative zone does not have permafrost conditions due to the formation of a talik (indicated by the empty symbol).

5 Rock glacier velocity

The kinematics of creeping permafrost landforms such as rock glaciers is primarily controlled by their intrinsic characteristics (e.g., internal structure and composition, topographical and geological settings), whereas changes over time are mainly driven by weather conditions, water availability and climate processes. Inter-annual changes in rock glacier velocity (RGV) mostly reflect the changes in the deformation rate at the shear horizon. The latter is typically located at 15–20 m depth within the permafrost body. This is where most of the deformation occurs (Cicoira et al. 2021). The velocity changes are related to the evolution of the ground temperature and liquid water content between the upper surface of the permafrost (i.e., the permafrost table) and the shear horizon. At inter-annual time scale, RGV was shown to follow an exponential relation with multi-annual ground surface temperature forcing (i.e., increasing ground surface temperatures lead to an increase in velocity and conversely, see Staub et al. 2016). RGV are also strongly dependent on the thickness of the snow cover in winter, which affects both ground temperature and water availability (i.e. Bast et al. 2024, Kenner et al. 2020). Given the global occurrence of rock glaciers and the sensitivity of their surface velocity to ground temperatures, RGV was adopted in 2021 as associated quantity to the ECV Permafrost by the WMO (see Hu et al. 2025 for a review).

The velocity of rock glacier also exhibits seasonal variations, which can be related to the seasonal variations of snow and ground temperature. Whereas the min/max amplitude is very diverse, ranging from 1:1.1 to 1:10 depending on the rock glacier, the seasonal kinematics always follow an almost similar behaviour with minimal velocities reached at the onset of the snowmelt season (around May) and the maxima in fall or at the beginning of the winter season (October-November).

Surface velocities of rock glaciers are measured by annual terrestrial geodetic surveys (TGS, Section 5.1) at the end of summer (August–October), as well as by permanently installed GNSS devices (Section 5.2). These two complementary methods allow to capture the seasonal velocity variations (permanent GNSS) and their spatially distributed inter-annual changes (TGS).

Figure 5.1. Differential GNSS device. Photo: R. Delaloye.

5.1 Annual rock glacier velocity

Annual TGS are performed using high precision differential GNSS or total stations. The positions of selected boulders (10–100 points per site covering the entire landform and stable areas nearby) are measured to calculate the surface velocity of the landform. Control points (i.e., points located on stable areas) are used to calibrate and adjust the measured positions with an average accuracy in the range of mm to cm. For each rock glacier, a set of reference points is defined amongst the monitored boulders based on their spatial distribution (i.e., located within the area of the rock glacier where surface displacements are dominantly related to permafrost creep), data quality and completeness. The reference points are used to compute site averages (Figures 5.2 and 5.3).

In 2024, TGS measurements were performed at 17 of the 18 surveyed rock glaciers. Measurements at Murtèl-Corvatsch (COR) were not possible due to safety issues caused by rockfall activity. At the observed sites results show that rock glacier velocities generally increased in all regions of the Swiss Alps (Figure 5.2). Compared to 2023, an average increase of +39% was observed in the Swiss Alps. Regional increases range from +13% in the Engadine to +47% in the Upper Valais. The maximum increase in 2024 was observed at Hungerlitaelli in the Upper Valais (HUT2, +77%), whereas the minimum increase in 2024 was observed at Gruben in the same region (GRU, +5%). The observed velocity change is consistent with the high GST and permafrost temperatures, which reflect the warm year 2024 (see Sections 2 and 3).

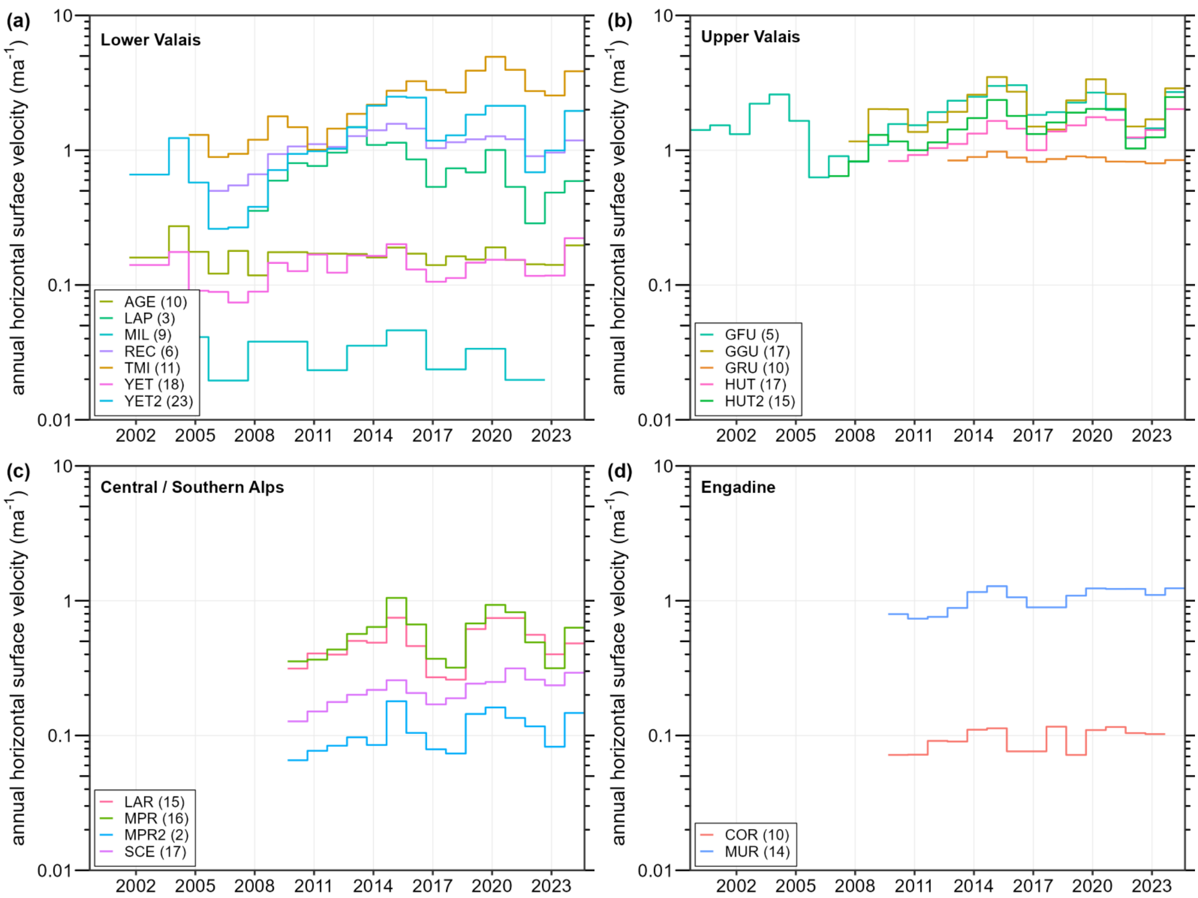

Figure 5.2. Pattern of horizontal surface velocities of 18 rock glacier lobes in the Swiss Alps, divided into four topo-climatic regions. The number of reference points for each site is indicated in brackets next to the site abbreviations (full site names can be found in Table 1.1).

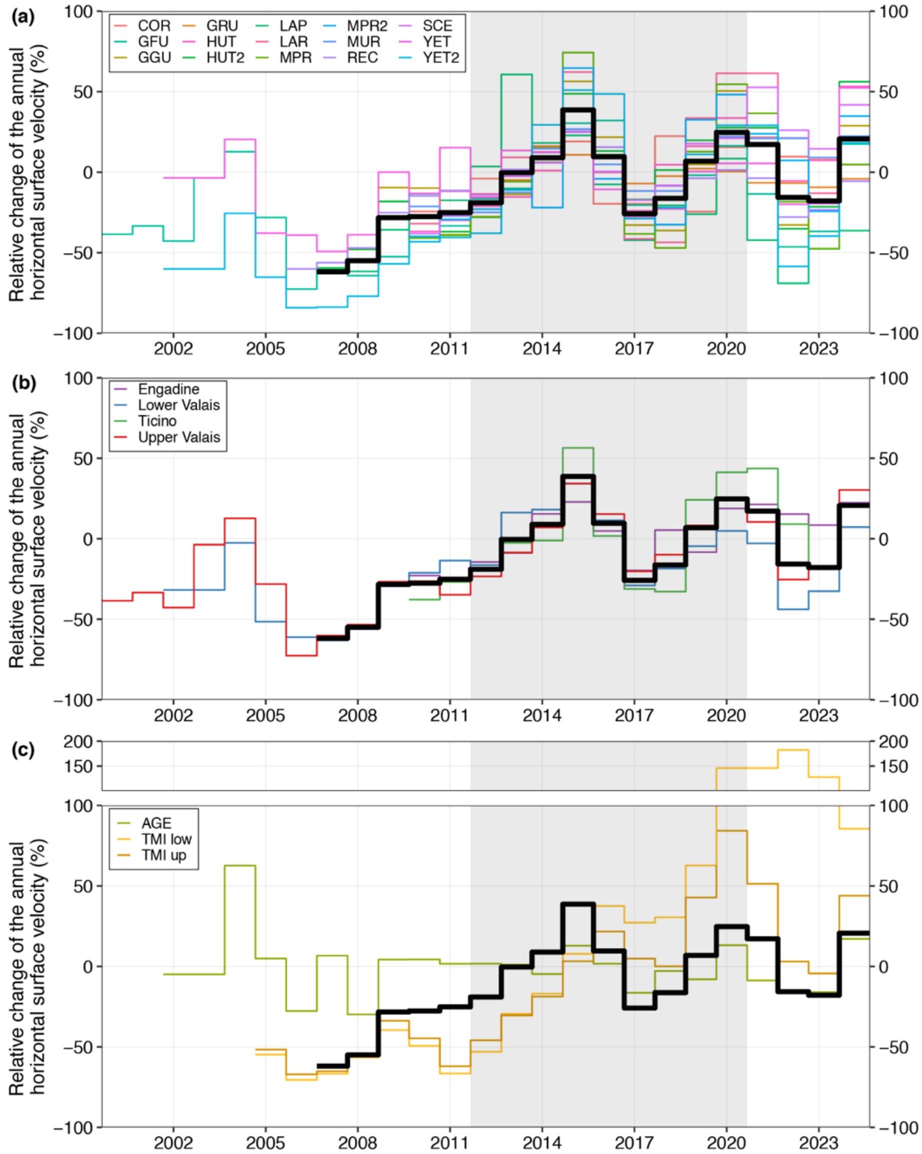

Figure 5.3. Mean annual horizontal surface velocity derived from terrestrial geodetic surveys relative to the reference period 2011–2020 (grey area). The black line is the average of all sites (excluding Tsarmine (TMI) and Aget (AGE)). (a) 15 monitored rock glacier lobes (for site abbreviations see Table 1.1). (b) Average for the four topo-climatic regions of the Swiss Alps. (c) Two atypical rock glaciers (note that TMI is divided into two separate areas).

Despite regional differences and variable landform size, morphology, and velocity range, a coherent evolution of rock glacier velocity can be identified in the Swiss Alps (Figure 5.3a). Since 2000, velocities have generally increased with marked inter-annual variability due to varying meteorological conditions. Periods of velocity decrease included 2004–2006, 2016–2018 and 2021–2022. Observed rates of velocity increase are highest since 2010 and maximum velocities were recorded in 2015 and/or 2020 depending on the site. Similar rock glacier velocity patterns have been reported in the French, Italian and Austrian Alps (Kellerer-Pirklbauer et al. 2024).

Two of the rock glaciers in the PERMOS Network do not follow this general pattern (Figure 5.3c). Since 2015, rock glacier Tsarmine (TMI) has been accelerating more strongly, especially in its lowermost part, while rock glacier Aget (AGE) has been decelerating from the start of the measurements in 2001 until around 2013. These contrasting kinematics are also interpreted as a response to climate warming: a deceleration typically results from in-situ permafrost degradation (i.e., thinning of the permafrost body above the shear horizon and/or increased friction at the shear horizon, e.g., due to freezing as a result of a snow-poor winter), whereas an exceptional acceleration points to an ongoing destabilization (see Roer et al. 2008). In both cases, these mechanisms overprint the general rock glacier evolution related to climate effects. In the case of Tsarmine, the surface velocities started to exhibit diverging behaviour since around 2015 between the upper and lower part of the rock glacier. While the upper part is moving faster than any of the observed rock glaciers (~3-5 m a^{-1}), its inter-annual evolution remains similar to the Swiss average, though with a larger variability. The lower part displayed a singular acceleration peaking around 2020–2022 with annual velocities of about 15 m $a^{-1}$and late autumn maxima exceeding 20 m a^{-1}. Scarps developed between the two different kinematic units due to the extension of the moving mass, which exceeds 70 m between both sections until 2024.

5.2 Seasonal rock glacier velocity

Permanent GNSS devices are installed on 8 rock glaciers of the PERMOS Network and deliver continuous position measurements. The raw GNSS data are post-processed using a double-difference processing scheme to obtain robust quality controlled daily positions. The high temporal resolution provided by permanent GNSS device enables the computation of monthly to daily displacements (depending on the absolute velocity of the rock glacier), which complement the annual TGS data presented in the previous section. Small velocity variations (smaller than ±0.1–0.2 m a^{-1}) must be interpreted with caution as they can be influenced by different factors (e.g. snow pressure on the GNSS mast in winter, stability of the boulder in the terrain) and, hence, are potentially not representative of the general rock glacier motion (e.g. Wirz et al. 2014). To ensure the reliability of velocity observations and to exclude such short-term variations, positions are filtered and aggregated with a 30-day moving window.

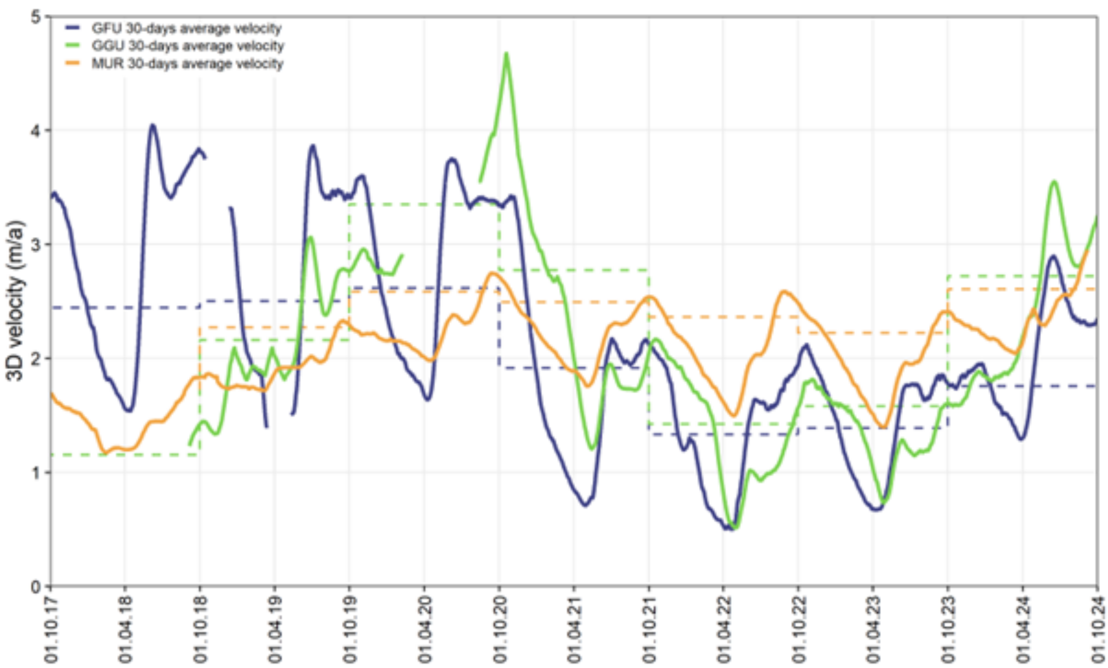

Figure 5.4. Evolution of the seasonal 3D surface velocity at the rock glaciers Gemmi (purple), Grosses Gufer (green) and Muragl (orange). The velocities are computed over 30-day periods. The dotted lines represent the annual surface velocity measured by TGS at the boulder closest to the GNSS device.

Figure 5.4 shows the seasonal evolution of surface velocities for three rock glaciers: Gemmi (GFU, Upper Valais), Grosses Gufer (GGU, Upper Valais) and Muragl (MUR, Engadine). A typical seasonal pattern can be observed at all sites: i) decreasing velocities in winter with minima in April followed by ii) a strong acceleration at the beginning of summer (during snow melt) and iii) peak velocities observed at the end of summer (when GST are the highest). The amplitude of the seasonal variations is variable and controlled by site-specific conditions (e.g. topography, geology, hydrology) as well as the local meteorological and snow conditions. The velocity decrease during winter partly depends on the intensity of the ground surface cooling.

During the hydrological year 2024 rock glacier velocities generally followed the typical seasonal pattern. The winter deceleration (cf. i above) was much less pronounced than in previous years at Gemmi and Muragl and hardly observed at Grosses Gufer. This is consistent with the minimal ground cooling observed near the surface during the snow-rich winter 2024 (Chapter 3.1). The acceleration following the snow melt period (cf. ii above) was higher than in 2023 at Gemmi and Grosses Gufer, reaching marked velocity peaks at the beginning of the summer. At Muragl, the acceleration was constant throughout the summer, and a velocity peak was reached in September. There, large amounts of water were observed in the rock glacier within the permafrost body during the drilling of 5 boreholes in August 2024. At Grosses Gufer and Gemmi the end of summer peak had not yet been reached on 1 October 2024. At the end of the hydrological year 2024, the velocities at all sites were clearly higher than at the beginning of October 2023. This confirms the higher annual average velocity observed by the terrestrial geodetical surveys (dashed lines in Figure 5.4).

6 Rock slope failures in permafrost in the calendar year 2024

Permafrost warming and degradation is expected to reduce the stability of perennially frozen slopes and lead to an increased probability of rock fall events. The stability of permanently frozen rock faces depends on various factors (e.g., Krautblatter et al. 2013; Gruber & Haeberli 2007; Jacquemart et al. 2024). The general predisposition of a slope to fail is determined by the geological structure (lithology, structure, fracturing) and the topography. Permafrost changes alter the variable predisposition (Fehlmann et al. 2016) and are related to a shorter-term fluctuation of the susceptibility of a rock slope to failure. Permafrost warming generally decreases the strength of the rock and ice-filled fissures (Mellor 1973; Davies et al. 2001; Mamot et al. 2021). Melt of permafrost ice in rock fractures can, for example, lead to deep-seated water infiltration, causing rapid temperature changes and increases in hydrostatic pressure (Hasler et al. 2011, Offer et al. 2025).

To assess and understand when and under what geological, thermal or topographical conditions rock slope failures (RSF) from permafrost areas occur, a permafrost RSF data base is maintained by the WSL Institute for Snow and Avalanche Research SLF in the framework of PERMOS. This documentation is a basis for scientific investigations. It includes and extends earlier compilations (Noetzli et al. 2003; Fischer et al. 2012) and evolved continuously in the past decades. The data are checked and supplemented with new information from satellite imagery, drone flights, terrestrial photographs and reports. The criteria for an event to be included are i) the starting zone is in a permafrost area and ii) the volume is larger than 1000 m^3. Key data sources are media reports and information from people active in the high mountain terrain, such as mountain guides, hut wardens, mountaineers, researchers or hazard managers. The list of events with the most complete information is accessible via the PERMOS Data Portal. As there is no operational Swiss rock fall observer network, the documentation is subject to a considerable observer bias. Large rock slope failures such as bergsturz events are well documented. The quality of information on events with smaller volumes is significantly lower. In addition, a boom in recreational mountain activities, the availability of mobile devices and awareness of the topic have increased in recent decades, which is likely to lead to more reports and better data quality.

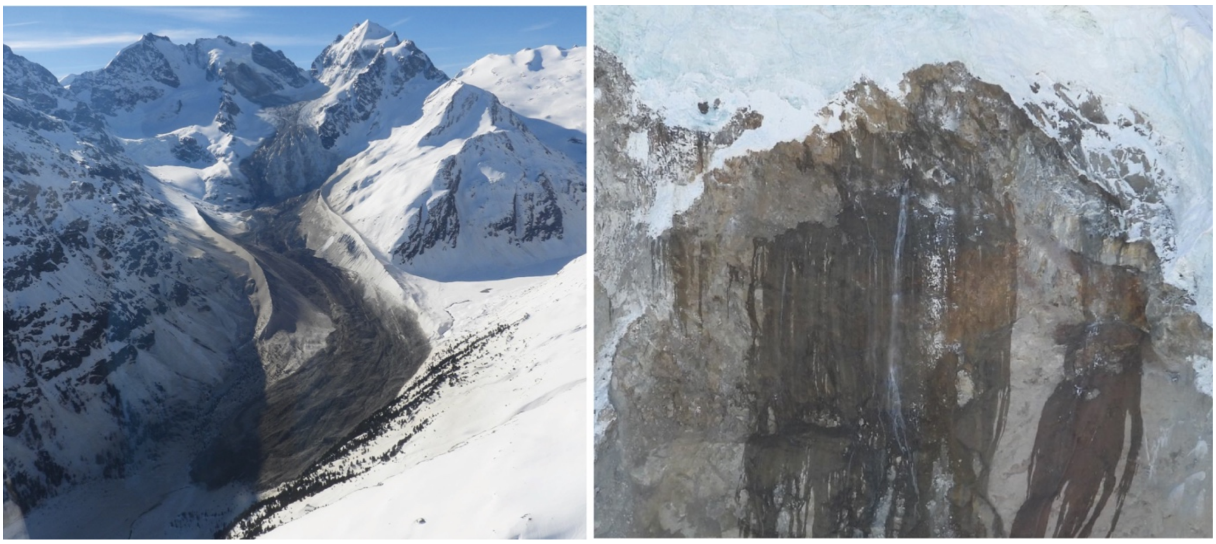

Figure 6.1. Bergsturz from Piz Scerscen on 14 April 2024. left: The rock and ice masses travelled almost 6 km over the Tschierva glacier (photo: M. Pasini). Right: Some ice and a waterfall were visible in the starting zone immediately after the event (photo: D. Hunziker).

The rockfall season 2024 started with a bang on 14 April, when around 5 million m^3 of rock collapsed in the Western flank of Piz Scerscen, Canton Grisons (Figure 6.1). The rock masses eroded and entrained large quantities of snow and ice and flowed over 5 km into the Val Roseg (Pierhöfer et al. 2024). Fortunately, no lives were lost, and no infrastructure was damaged. Large quantities of water poured out of the detachment zone at 3660 m asl. for several hours from a water pocket located within the frozen rock mass, with estimated rock temperatures of around –5 °C. It is likely that the water accumulated in the previous hot summers and water pressure contributed to triggering this impressive bergsturz.

On June 21 a rock slope failure with an estimated volume of around 100’000 m^3 (data source: Guardaval/Canton VS) was observed on the southeastern flank of the Grand Portalet VS, in the zone named Ravines Rousses. The detachment zone was not located in permafrost but close to its lower limit.

Relatively little rockfall was observed thereafter until mid-August, when several medium sized events were observed, with volumes of thousands to tens of thousands of cubic metres, mainly in the Valais and central Alps. They mainly occurred during periods with high air temperatures followed by rainfall. The autumn season was marked by large rock avalanches, for example the collapse of the Tschingelhorn ridge (with a volume of 100’000 m^3) above the Martinsloch (GR/GL) on 3 October 2024 or a series of large events on the Dent de Pro (VS) in November with a total volume of over 150’000 m^3 on both sides of the ridge. The location of the latter events is interesting, as they are very close to the large rock slope failures which occurred at the Col de Tseudet in 1967 and in 2020/2021. At the end of December, a rock slope failure of ca. 70’000 m^3 occurred on the Klein Aletschhorn, followed by a large RSF at the Swiss-Italian border on Colle Signal, which entrained snow and ice and flowed over the Italian Belvedere glacier. Although many other events were reported in 2024, the completeness of information needs to be improved before integration into the PERMOS data base.

7 Conclusions

The Swiss Permafrost Monitoring Network PERMOS documents the state and changes of permafrost in the Swiss Alps based on field measurements of ground temperatures, electrical resistivities and rock glacier velocities. All observations show a consistent pattern of continued warming and permafrost degradation in the Swiss Alps since the start of PERMOS in 2000. The general trend is overlaid by inter-annual variations in response to annual meteorological conditions, particularly the timing and depth of the snow cover and air temperatures.

The hydrological year 2024 was characterized by a very mild and snow-rich winter, a cool and wet spring, and very warm atmospheric conditions in summer and autumn 2024. It was the second warmest hydrological year in Switzerland above 1000 m asl. since the start of the measurements in 1864 (the calendar year 2024 was the third warmest year). These climate conditions led to the following conditions in the permafrost in the Swiss Alps (Figure 7.1):

- Ground surface temperatures remained at high levels and reached record levels at more than half of the sites observed. Record running mean annual ground surface temperatures were reached in spring 2024 following a very warm winter at the ground surface due to the early and abundant snow fall in autumn 2023.
- Record high active layer thicknesses (ALT) were observed in 2024 for all boreholes in which it could be determined. The ALT at all three boreholes on Schilthorn no longer refroze in winter 2024, thus confirming the formation of a talik and permafrost degradation.
- Permafrost temperatures at 10 m depth increased in 2024 compared to 2023 by a few tenths of degrees Celsius at all sites and reached new maximum values. The warm, snow-rich winter considerably contributed to this warming.
- Permafrost electrical resistivities continued to decrease considerably at the high-elevation bedrock site Stockhorn and the talus slope Lapires. At Schilthorn, a resistivity increase in the recently developed talik was observed. This points to a drying of the thaw layer at the site.
- Rock glacier velocity increased at all surveyed sites with an average of +39% over the Swiss Alps compared to 2023. Regional increases ranged from +13% in the Engadine to +47% in the Upper Valais. Seasonal velocity observations show that this general acceleration of annual velocity is for a large part due to the less pronouced winter deceleration.
- The 2024 rockfall season began with a 5 Mio. m^3 rock slope failure at Piz Scerscen, entraining large quantities of snow and ice and with a runout of over 5 km. After a quieter period, rockfall activity resumed in mid-August and autumn with several larger events (>100’000 m^3) across the Alps.

Overall, the permafrost observations during the hydrological year 2024 point to very warm and mostly record warm permafrost conditions in the Swiss Alps for all measured key variables: ground surface temperatures, active layer thickness, permafrost temperature, permafrost resistivity and rock glacier velocity.

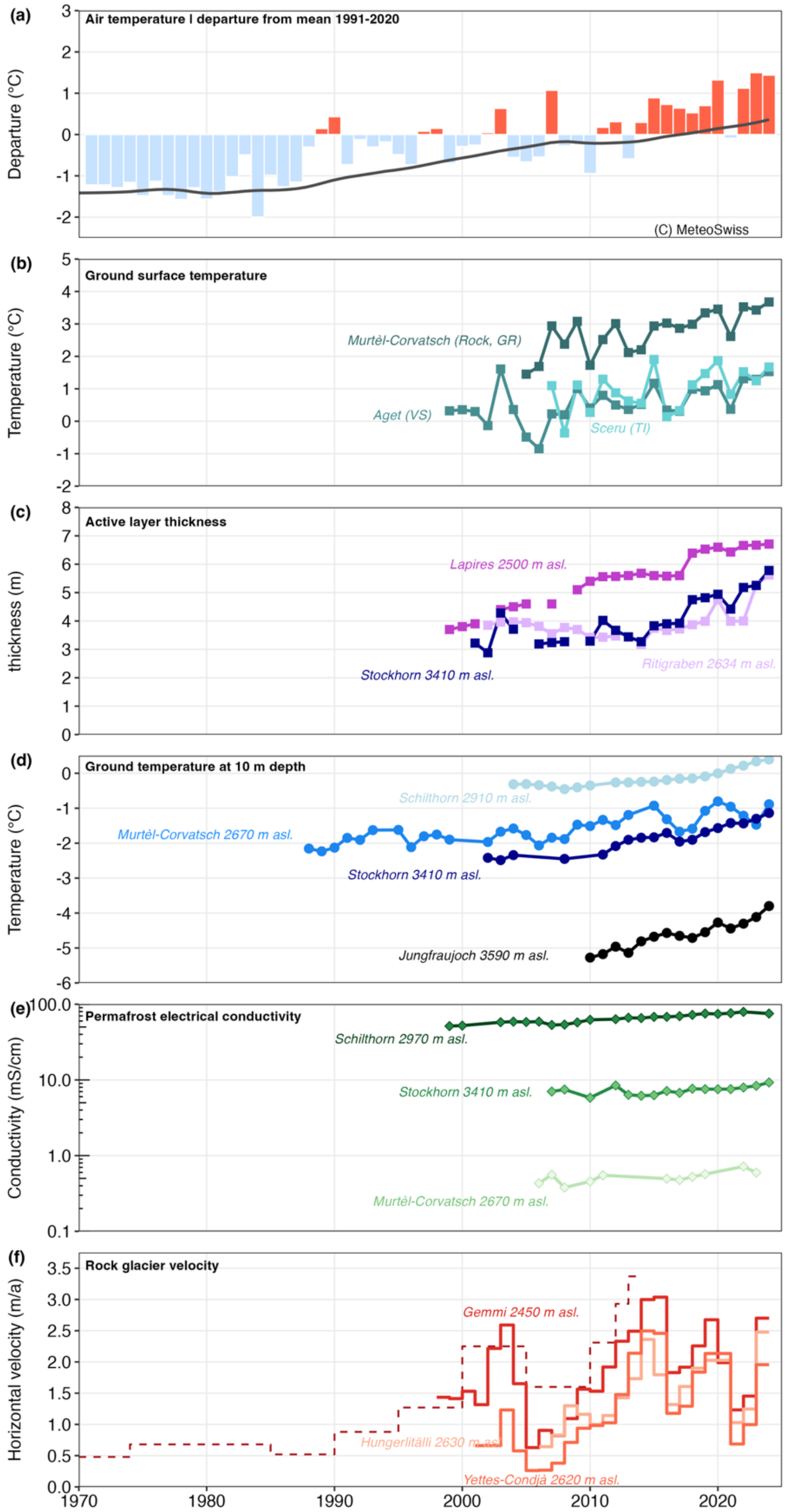

Figure 7.1. Evolution of the key observation elements of the Swiss permafrost monitoring and anomaly of annual air temperatures to the 1991–2020 climate norm period (a, data source: MeteoSwiss, homogenized data series for Swiss stations above 1000 m asl.): Mean annual ground surface temperature (b), active layer thickness (c), annual mean permafrost temperatures at 10 m depth (d), permafrost electrical conductivity (e), and rock glacier creep velocity (f). The dashed red line represents the horizontal surface velocity for rock glacier Gemmi obtained by aerial photogrammetry. All annual mean values relate to the hydrological years (October–September).

Acknowledgements

The site installation and maintenance, fieldwork and data preprocessing were performed by the seven partner institutions of the Swiss Permafrost Monitoring Network PERMOS: The Swiss Federal Institute of Technology (ETH Zurich) through their Laboratories of Hydraulics, Hydrology and Glaciology (VAW), the WSL Institute for Snow and Avalanche Research SLF, the University of Applied Sciences and Arts of Southern Switzerland (SUPSI) through their Institute of Earth Sciences, the University of Lausanne through the Institute of Earth Surface Dynamics, the University of Innsbruck through the Institute of Informatics, and the Geography Departments of the Universities of Fribourg and Zurich. The Swiss Permafrost Monitoring Network is financially supported by MeteoSwiss, in the framework of GCOS Switzerland, the Federal Office for the Environment FOEN and the Swiss Academy of Sciences SCNAT.

References

Bast, A., Kenner, R., and Phillips, M. 2024. Short-term cooling, drying, and deceleration of an ice-rich rock glacier. The Cryosphere, 18(7), 3141–3158. https://doi.org/10.5194/tc-18-3141-2024.

Cicoira, A., Marcer, M., Gärtner-Roer, I., Bodin, X., Arenson, L.U. and Vieli, A. 2021. A general theory of rock glacier creep based on in-situ and remote sensing observations. Permafrost and Periglacial Processes, 32, 139–153, doi.org/10.1002/ppp.2090.

Davies, M.C.R., Hamza, O. and Harris, C. 2001. The effect of rise in mean annual temperature on the stability of rock slopes containing ice-filled discontinuities. Permafrost and Periglacial Processes, 12, 137–144, doi.org/10.1002/ppp.378.

Fehlmann, M., Mani, P. and Stoffel, M. 2016. Der Einfluss des Klimas auf Steinschlag im periglazialen Prozessbereich der Alpen. FAN Herbstkurs 2016, 25–31.

Fischer, L., Purves, R.S., Huggel, C., Noetzli, J. and Haeberli, W. 2012. On the influence of topographic, geological and cryospheric factors on rock avalanches and rockfalls in high-mountain areas. Natural Hazards and Earth System Sciences, 12, 241–254, doi.org/10.5194/nhess-12-241-2012.

Gruber, S. and Haeberli, W. 2007. Permafrost in steep bedrock slopes and its temperature-related destabilization following climate change. Journal of Geophysical Research, 112, doi.org/10.1029/2006JF000547.

Hasler, A., Gruber, S., Font, M. and Dubois, A. 2011. Advective Heat Transport in Frozen Rock Clefts: Conceptual Model, Laboratory Experiments and Numerical Simulation. Permafrost and Periglacial Processes, 22, 378–389, doi.org/10.1002/ppp.737.

Hoelzle, M., Hauck, C., Mathys, T., Noetzli, J., Pellet, C. and Scherler, M. 2022. Long-term energy balance measurements at three different mountain permafrost sites in the Swiss Alps. Earth System Science Data, 14, 1531–1547, doi.org/10.5194/essd-14-1531-2022.

Hu, Y.; Arenson, L.U.; Barboux, C., Bodin, X., Cicoira, A., Delaloye, R., Gärtner-Roer, I., Kääb, A., Kellerer-Pirklbauer, A., Lambiel, C., Liu, L., Pellet, C., Rouyet, L., Schoeneich, P., Seier, G. and Strozzi, T. 2025. Rock Glacier Velocity: An Essential Climate Variable Quantity for Permafrost. Reviews of Geophysics, 63, e2024RG000847, doi:10.1029/2024RG000847.

Jacquemart, M., Weber, S., Chiarle, M., Chmiel, M., Cicoira, A., Corona, C., Eckert, N., Gaume, J., Giacona, F., Hirschberg, J., Kaitna, R., Magnin, F., Mayer, S., Moos, C., Van Herwijnen, A. and Stoffel, M. 2024. Detecting the impact of climate change on alpine mass movements in observational records from the European Alps. Earth-Science Reviews 258, 104886, doi.org/10.1016/j.earscirev.2024.104886.

Kellerer-Pirklbauer, A., Bodin, X., Delaloye, R., Lambiel, C., Gärtner-Roer, I., Bonnefoy-Demongeot, M., Carturan, L., Damm, B., Eulenstein, J., Fischer, A., Hartl, L., Ikeda, A., Kaufmann, V., Krainer, K., Matsuoka, N., Morra Di Cella, U., Noetzli, J., Seppi, R., Scapozza, C., Schoeneich, P., Stocker-Waldhuber, M., Thibert, E. and Zumiani, M. 2024. Acceleration and interannual variability of creep rates in mountain permafrost landforms (rock glacier velocities) in the European Alps in 1995–2022. Environmental Research Letters 19, 034022, doi.org/10.1088/1748-9326/ad25a4

Kenner, R., Pruessner, L., Beutel, J., Limpach, P., and Phillips, M. 2020. How rock glacier hydrology, deformation velocities and ground temperatures interact: Examples from the Swiss Alps. Permafrost and Periglacial Processes, 31(1), 3–14. https://doi.org/10.1002/ppp.2023.

Krautblatter, M., Funk, D. and Günzel, F.K. 2013. Why permafrost rocks become unstable: a rock-ice-mechanical model in time and space. Earth Surface Processes and Landforms, 38, 876–887, doi.org/10.1002/esp.3374.

Mamot, P., Weber, S., Eppinger, S. and Krautblatter, M. 2021. A temperature-dependent mechanical model to assess the stability of degrading permafrost rock slopes. Earth Surface Dynamics, 1125–1151.

Mellor, M. 1973. Mechanical properties of rocks at low temperatures. In Proceedings. 2nd International Conference on Permafrost. Yakutsk, pp. 334–344.

Mollaret, C., Hilbich, C., Pellet, C., Flores-Orozco, A., Delaloye, R. and Hauck, C. 2019. Mountain permafrost degradation documented through a network of permanent electrical resistivity tomography sites. The Cryosphere 13, 2557–2578, doi.org/10.5194/tc-13-2557-2019.

MeteoSwiss 2025. Klimabulletin Jahr 2024. 16 pp., Zurich.
MeteoSwiss 2024. Klimabulletin Jahr 2023. 13 pp, Zurich.

Noetzli, J., Arenson, L.U., Bast, A., Beutel, J., Delaloye, R., Farinotti, D., Gruber, S., Gubler, H., Haeberli, W., Hasler, A., Hauck, C., Hiller, M., Hoelzle, M., Lambiel, C., Pellet, C., Springman, S.M., Vonder Muehll, D. and Phillips, M. 2021. Best Practice for Measuring Permafrost Temperature in Boreholes Based on the Experience in the Swiss Alps. Frontiers in Earth Science 9, 607875, doi.org/10.3389/feart.2021.607875.

Noetzli, J., Hoelzle, M. and Haeberli, W. 2003. Mountain permafrost and recent Alpine rock-fall events: a GIS-based approach to determine critical factors. In: 8th International Conference on Permafrost. 8th International Conference on Permafrost. Zurich, Switzerland, 827–832.

Noetzli, J., Isaksen, K., Barnett, J., Christiansen, H., Delaloye, R., Etzelmuller, B., Farinotti, D., Gallemann, T., Guglielmin, M., Hauck, C., Hilbich, C., Hoelzle, M., Lambiel, C., Magnin, F., Oliva, M., Paro, L., Pogliotti, P., Riedl, C., Schoeneich, P., Valt, M., Vieli, A. and Phillips, M. 2024. Enhanced warming of European mountain permafrost in the early 21st century. Nature Communications, doi.org/10.1038/s41467-024-54831-9.

Noetzli, J., Peter, A., Hählen, N. and Phillips, M. 2025. Verborgenes Eis in den Schweizer Alpen: Der Permafrost taut immer schneller. In: Forum für Wissen 2025: Extremes (WSL Berichte 164). Forum für Wissen 2025: Extremes. Swiss Federal Institute for Forest, Snow and Landscape Research, WSL, 35–47, doi.org/10.55419/wsl:39741.

Offer, M., Weber, S., Krautblatter, M., Hartmeyer, I. and Keuschnig, M. 2025. Pressurised water flow in fractured permafrost rocks revealed by borehole temperature, electrical resistivity tomography, and piezometric pressure. The Cryosphere, 19, 485–506, doi.org/10.5194/tc-19-485-2025.
PERMOS 2019. Permafrost in Switzerland 2014/2015 to 2017/2018. Noetzli, J., Pellet, C. and Staub, B. (eds.), Glaciological Report Permafrost No. 16–19 of the Cryospheric Commission of the Swiss Academy of Sciences, 104 pp, doi.org/10.13093/permos-rep-2019-16-19.

Pierhöfer, L., Bartelt, P., Bühler, Y., Hafner, E., Kenner, R., Walter, F., and Phillips, M. 2025. Bergsturz vom 14. April 2024 am Piz Scerscen, Graubünden. Swiss Federal Institute for Forest, Snow and Landscape Research, WSL, doi.org/10.55419/wsl:38392.

Roer, I., Haeberli, W., Avian, M., Kaufmann, V., Delaloye, R., Lambiel, C. and Kääb, A. 2008. Observations and considerations on destabilizing active rock glaciers in the European Alps. In: 9th International Conference on Permafrost. 9th International Conference on Permafrost. Fairbanks, US, 1505–1510.

Staub, B., Hasler, A., Noetzli, J. and Delaloye, R. 2017. Gap-Filling Algorithm for Ground Surface Temperature Data Measured in Permafrost and Periglacial Environments. Permafrost and Periglacial Processes, 28, 275–285, doi.org/10.1002/ppp.1913.

Staub, B., Lambiel, C. and Delaloye, R. 2016. Rock glacier creep as a thermally-driven phenomenon: A decade of inter-annual observation from the Swiss Alps. In: Proceedings of the 9th International Conference on Permafrost, Potsdam, Germany, 96–97.

Streletskiy, D., Noetzli, J., Smith, S.L., Vieira, G., Schoeneich, P., Hrbacek, F. and Irrgang, A.M. 2021. Strategy and Implementation Plan for the Global Terrestrial Network for Permafrost (GTN-P) 2021–2024, doi.org/10.5281/ZENODO.6075468.

Wirz, V., Beutel, J., Gruber, S., Gubler, S. and Purves, R.S. 2014. Estimating velocity from noisy GPS data for investigating the temporal variability of slope movements. Natural Hazards and Earth System Sciences, 14, 2503–2520, doi.org/10.5194/nhess-14-2503-2014.

WMO 2017. WMO guidelines on the calculation of climate normals. World Meteorological Organization WMO, No. 1203, 18 pp. Geneva, Switzerland.

WMO 2022. The 2022 GCOS ECV Requirements. World Meteorological Organization (WMO), United Nations Educational, Scientific and Cultural Organization, Intergovernmental Oceanographic Commission, United Nations Environment Programme, International Science Council (ISC), GCOS No. 245, 261 pp., Geneva, Switzerland.

WMO 2024. Guide to meteorological instruments and methods of observation, Geneva: World Meteorological Organization, doi.org/10.59327/WMO/CIMO/2.

Zweifel B., Techel F., Marty C. and Stucki T. 2024. Schnee und Lawinen in den Schweizer Alpen. Hydrologisches Jahr 2023/24. WSL Bericht 145, 84 pp, doi.org/10.55419/wsl:3852.